



1 **Wet deposition in the remote western and central**  
2 **Mediterranean as a source of trace metals to surface seawater**

Commented [RS(-S1)]: Could be more descriptive

3 Karine Desboeufs<sup>1</sup>, Franck Fu<sup>1</sup>, Matthieu Bressac<sup>2,3</sup>, Antonio Tovar-Sánchez<sup>4</sup>, Sylvain Triquet<sup>1</sup>,  
4 Jean-François Doussin<sup>5</sup>, Chiara Giorio<sup>6,7</sup>, Patrick Chazette<sup>8</sup>, Julie Disnaquet<sup>9,10</sup>, Anaïs Feron<sup>1</sup>,  
5 Paola Formenti<sup>1</sup>, Franck Maisonneuve<sup>5</sup>, Araceli Rodríguez-Romero<sup>4</sup>, Pascal Zapf<sup>5</sup>, François Dulac<sup>8</sup>  
6 and Cécile Guieu<sup>3</sup>

7 <sup>1</sup> Université de Paris and Univ Paris Est Creteil, CNRS, LISA, UMR 7583, F-75013 Paris, France

8 <sup>2</sup> Institute for Marine and Antarctic Studies, University of Tasmania, Hobart, Tasmania, Australia.

9 <sup>3</sup> Laboratoire d'Océanographie de Villefranche (LOV), CNRS-Sorbonne Université, INSU, Villefranche-sur-Mer, 06230,  
10 France.

11 <sup>4</sup> Department of Ecology and Coastal Management, Institute of Marine Sciences of Andalusia (CSIC), 11510 Puerto Real,  
12 Cádiz, Spain.

13 <sup>5</sup> Univ Paris Est Creteil and Université de Paris, CNRS, LISA, UMR 7583, F-94010 Créteil, France

14 <sup>6</sup> Laboratoire de Chimie de l'Environnement (LCE), UMR 7376 CNRS, Aix-Marseille Université, Marseille, 13331,  
15 France.

16 <sup>7</sup> Yusuf Hamied Department of Chemistry, University of Cambridge, Lensfield Road, CB2 1EW, Cambridge, United  
17 Kingdom

18 <sup>8</sup> Laboratoire des Sciences du Climat et de l'Environnement (LSCE), UMR 8212 CEA-CNRS-UVSQ, Institut PierreSimon  
19 Laplace, Univ. Paris-Saclay, 91191 Gif-sur-Yvette, France.

20 <sup>9</sup> Marine Biology Research Division, Scripps Institution of Oceanography, UCSD, USA

21 <sup>10</sup> Sorbonne Université, CNRS, Laboratoire d'Océanographie Microbienne, LOMIC, France

22

23

24 *Correspondence to:* Karine Desboeufs (karine.desboeufs@lisa.ipsl.fr)

25

26

27

28

29

30

31 **Abstract.** This study reports the only recent characterisation of two contrasted wet deposition events  
32 collected during the PEACETIME cruise in the open Mediterranean Sea open seawater, and their



33 impact on trace metals (TMs) marine stocks. Rain samples were analysed for Al, 12 ~~trace metals (TMs)~~  
34 ~~hereafter, including~~ (Co, Cd, Cr, Cu, Fe, Mn, Mo, Ni, Pb, Ti, V and Zn) and nutrients (N, P, DOC)  
35 ~~concentrations~~. The first rain sample collected in the Ionian Sea (~~rain~~-Rain ION) was a ~~wet~~-typical  
36 regional background wet deposition event whereas the second rain sample, collected in the Algerian  
37 Basin (Rain FAST), was a Saharan dust wet deposition event. The concentrations of TMs in the two  
38 rain samples were significantly lower compared to concentrations in rains collected at coastal sites  
39 reported in the literature, suggesting either less anthropogenic influence in the remote Mediterranean  
40 ~~environment~~Sea, or decreased anthropogenic emissions during the last-preceding decades ~~in the~~  
41 ~~Mediterranean Sea~~. The TMs inventories in the surface microlayer and mixed layer (0-20\_m) at ION  
42 and FAST stations before and after the events were, compared to atmospheric fluxes which, showed  
43 that the atmospheric inputs were a significant source of particulate TMs for both layers. At the scale  
44 of the western and central Mediterranean, the atmospheric inputs were of the same order of magnitude  
45 as marine stocks within the ML for dissolved Fe, Co and Zn, underlining-highlighting the role of the  
46 atmosphere in their biogeochemical cycles in the stratified Mediterranean Sea (state season) under  
47 background conditions (?). ~~In case of~~Our results suggest that -intense dust-rich wet dust deposition  
48 ~~events, are an important source-the contribution of atmospheric inputs could be critical for~~ of dissolved  
49 ~~stocks of the majority of TMs to the study region~~.

Commented [RS(-S2)]: Already defined if rewording is accepted.

Commented [RS(-S3)]: define

Commented [RS(-S4)]: Not yet defined



## 51 1. Introduction

52 Atmospheric deposition of ~~continental aerosol~~ has long been recognized to influence trace element  
53 ~~(TE)~~ concentrations in remote oceanic surface waters (Buat-Ménard and Chesselet, 1979; Hardy,  
54 1982; Buat-Ménard, 1983). In particular, the Mediterranean Sea (Med Sea) is an oligotrophic  
55 environment where marine ~~biosphere~~ growth is ~~nutrient-limited~~ during the long Mediterranean  
56 summer season, ~~which is~~ characterized by a strong thermal stratification of surface waters (The  
57 Mermex Group, 2011). The Mediterranean atmosphere is characterized by the permanent presence of  
58 anthropogenic aerosols from industrial and domestic activities around the basin (e.g., Sciare et al.,  
59 2003; Kanakidou et al., 2011). In addition to this anthropogenic background, the Mediterranean basin  
60 is also subject to seasonal contributions of particles from biomass fires in summer (Guieu et al., 2005)  
61 and to intense sporadic Saharan dust inputs (e.g., Loÿe-Pilot and Martin, 1996; Vincent et al., 2016).  
62 Several studies ~~have~~ emphasized that the atmospheric deposition of aerosols, notably through wet  
63 deposition, plays a significant role in ~~the~~ marine cycles of ~~both~~-nutrients, such as nitrogen (N) and  
64 phosphorus (P) (e.g. Pulido-Villena et al., 2010; Richon et al., 2018 a and b; Violaki et al., 2018) and  
65 micronutrients, such as iron (Fe) (Bonnet and Guieu, 2006). Recently, atmospheric dust inputs were  
66 identified to have a fertilizing effect on ~~the~~-planktonic stocks and fluxes, even in the presence of  
67 relatively high ~~dissolved ()~~nutrients-N, P and Fe ~~marine~~-concentrations (Ridame et al., 2011; reviewed  
68 in Guieu and Ridame, 2021). Mackey et al. (2012) showed that TMs provided by dust deposition could  
69 explain this fertilizing effect. Indeed, ~~some-many~~ TMs, including Mn, Co, Ni (Mackey et al., 2012),  
70 Cu (Annett et al., 2008) and Zn (Morel et al., 1991), play physiological roles for phytoplanktonic  
71 organisms. These TMs are present in very low concentrations in oligotrophic systems such as the Med  
72 Sea, possibly limiting ~~(or co-limiting) the~~-phytoplankton growth (Pinedo-González et al. 2015), ~~and~~  
73 ~~implying the role~~pointing to the importance of dust deposition as source of TMs for planktonic  
74 communities. On the other hand, atmospheric deposition of European aerosol-~~particleless~~ was identified  
75 to have a negative effect on chlorophyll concentrations (Gallissai et al. 2014), by providing ~~trace~~  
76 ~~metals, as~~-Cu, at toxic levels (Jordi et al. 2012).

77 The atmospheric deposition of TMs in the Mediterranean is related to both dust and anthropogenic  
78 aerosol-~~s~~ deposition (Desboeufs et al., 2018). The role of dust deposition as a source of TMs was  
79 observed from the correlation between the atmospheric deposition of mineral dust, and the enrichment  
80 of dissolved TMs (Cd, Co, Cu, Fe) in the Mediterranean Sea surface microlayer (Tovar Sánchez et al.,  
81 2014). For the water column, the adding of dissolved Fe and Mn was emphasized in mesocosm  
82 experiments after dust addition mimicking intense wet dust deposition (Wuttig et al., 2013). ~~Yet, the~~  
83 ~~direct impact of wet deposition events~~-on TMs concentrations in surface seawater has ~~never-not~~ been  
84 ~~studied and reported in-situ where TM concentrations were determined in both rainwater and seawater~~  
85 ~~samples collected from the same location before the present study, whether in the Mediterranean Sea~~

Commented [RS(-S5)]: Define/give examples

Commented [RS(-S6)]: Replace with microbial. Biosphere is too general

Commented [RS(-S7)]: Which nutrients?



86 or in other oceanic regions. Moreover, the two key criteria used to assess the potential impact of TMs  
87 and nutrients wet deposition ~~are and~~ their respective concentrations (or fluxes) and solubility, i.e., the  
88 partitioning between dissolved and total concentrations in rainwaters. Indeed, it is considered that the  
89 dissolved fraction of nutrients and TMs can be directly assimilated by the phytoplankton (ref). A few  
90 studies ~~have focussed on reported~~ concentrations of  
91 TMs in rainwater samples ~~was~~ collected around the Mediterranean basin: Al-Momani et al., (1998),  
92 Kanellopoulou, (2001) and Özsoy and Örnektekin, (2009) in the eastern basin, and Losno (1989),  
93 Guieu et al. (1997), Frau et al., (1996), Chester et al., (1997) and Guerzoni et al. (1999b) in the western  
94 basin. These studies led to highly variable TMs concentrations and solubility, illustrating ~~a more~~  
95 ~~general~~ the large variability of TMs inputs during wet deposition ~~events~~ in the Mediterranean Sea  
96 (reviewed in Desboeufs, 2021). All these studies were performed at coastal sites. Offshore samples of  
97 rainwater have rarely been ~~studied reported~~ in the literature ~~so far~~. In the Mediterranean, to our  
98 knowledge, trace element concentrations from only three rain samples collected at sea in April 1981  
99 have been reported in a PhD thesis (Dulac, 1986). ~~However, due to the continental and local sources~~  
100 ~~of pollution and the variety of anthropogenic aerosol sources (Amato et al., 2016), the TMs rain~~  
101 ~~composition of the coastal zone could may~~ not be representative of atmospheric deposition ~~in to the~~  
102 ~~remote Mediterranean.~~

Commented [RS(-S8)]: To the best of our knowledge....

103 The PEACETIME cruise (ProcEss studies at the Air-sEa Interface after dust deposition in the  
104 MEditerranean Sea) performed in spring 2017 aimed ~~at to study~~ the impacts of atmospheric  
105 deposition, in particular Saharan dust events, on the physical, chemical and biological processes in  
106 this marine oligotrophic environment (Guieu et al., 2020). We investigated ~~here~~ the concentration and  
107 solubility of TMs and nutrients ~~of from~~ two rain ~~events waters~~ sampled in the ~~open~~ Mediterranean  
108 ~~open S~~ sea during the cruise. We compare our results ~~on of~~ TMs concentrations and solubility in  
109 rainwater with previous studies based on rainwater samples collected at coastal sites to investigate  
110 potential differences with the open sea. Additionally, to assess the impact of wet deposition on the  
111 surface TMs concentrations, surface seawater, including the surface micro-layer, ~~and rain water~~ was  
112 concurrently collected. ~~To the best of our knowledge, this is the first time TM data for these marine~~  
113 ~~compartments have all been presented at the same time. for the first time~~ with ~~rain samples.~~

Commented [RS(-S9)]: Coastal atmospheric TM concentrations are not usually representative of open ocean concentrations due to deposition of material en route

Commented [RS(-S10)]: It's definitely not the first time this has been done but might be the first time the data has been reported in the same place

Formatted: Strikethrough

## 114 2. Sampling and methods

### 115 2.1 Sampling and chemical analysis of rainwater

116 The PEACETIME oceanographic campaign (<https://doi.org/10.17600/17000300>) took place in the  
117 western and central Mediterranean Sea on-board the French research vessel ~~(R/V)~~ *Pourquoi Pas ?*  
118 between 11 May and 10 June 2017, i.e. at the beginning of the Mediterranean stratification season  
119 (Guieu et al., 2020). The rain collector was installed on the upper deck (22 m above sea level) where



120 no on-board activities were taking place to avoid contamination. ~~A-The~~ rain collector was equipped  
121 with an on-line filtration system to ~~directly~~ separate the dissolved and particulate fractions ~~at the time~~  
122 ~~of collection~~ (details of the filtration system are available in Heimbürger et al., 2012) allowing for the  
123 calculation of solubility of TMs in the rainwater ~~at the time of collection~~. The filtration device was  
124 equipped with a Nuclepore® polycarbonate membrane ~~(PC)~~ filter (porosity: 0.2 µm, diameter: 47  
125 mm). ~~I, and~~ the diameter of the funnel of the collector was 24 cm. ~~The rain collectors were was~~  
126 ~~installed opened~~ only when rain was expected and kept ~~closed within covered by~~ an acid-washed,  
127 sealed plastic film ~~until the rainfall began when not in use~~. All the sampling materials were thoroughly  
128 acid-washed in the laboratory prior to the cruise departure (washing protocol described in Heimbürger  
129 et al., 2012). No stabilizing ~~setup device~~ was used to keep the funnel level during the pitch and roll of  
130 the ship, preventing a precise assessment of the height of rainfall from the collected water volume.  
131 During the rain sampling, the ship was always facing the wind to avoid contamination by the ~~smoke~~  
132 ~~ship's exhaust of the ship itself~~, as the chimney was situated on the lower deck and behind the  
133 collector.

134 Immediately after sampling, the collector was disassembled under ~~the a~~ laminar flow hood inside an  
135 ~~on-board~~ clean-room ~~on board~~ laboratory. The dissolved fraction was separated into ~~to 4-four~~ aliquots  
136 dedicated to i) dissolved organic carbon (DOC) ~~determination~~ by high-temperature catalytic  
137 oxidation (HTCO) on a Shimadzu total organic carbon analyzer (as described in Van Wambeke et al  
138 2021), ii) major ions by ion chromatography (IC), ~~iii) metals analysis~~ ~~TM determination~~ by inductively  
139 coupled plasma ~~coupled~~ methods (ICP), and iv) pH measurement. For ICP measurements, the sample  
140 was acidified immediately to 1% by volume of ultra-pure nitric acid: 67-69%, Ultrapur, Normatom®,  
141 VWR. ~~For DOC analysis...~~ For IC analysis, the ~~filtrate sample (dissolved fraction)~~ was immediately  
142 frozen. The filter (particulate fraction) was dried under the laminar flow hood, and then put in a storage  
143 box and packed with a plastic bag to avoid contamination. After returning to the laboratory, filters  
144 were acid digested by using the ~~adapted~~ protocol ~~adapted~~ from Heimbürger et al.  
145 (2012) as follows: filters were placed in tightly capped Savillex™ PFA digestion vessels with 4 mL  
146 of a mixture of HNO<sub>3</sub> (67-69%, Ultrapur, Normatom®, VWR), H<sub>2</sub>O and HF acids (40%, Ultrapur,  
147 Normatom®, VWR) in a proportion ~~of (3: 1: 0.5)~~, then heated in an oven at 130°C for 14 hours. After  
148 cooling, ~~the acid solution~~ was completely evaporated on a heater plate (ANALAB, 250, A4) at 140°C  
149 for about  
150 2h, then 0.5 mL of H<sub>2</sub>O<sub>2</sub> (30-32%, Romil-UpA™) and 1 mL of the acidified water (2% HNO<sub>3</sub>) was  
151 added to the vessels and heated ~~during for~~ 30 min. to dissolve the dry residue in the bottom of the  
152 vessels; finally, 12 mL of acidified water (1% HNO<sub>3</sub>) was added to obtain 13.5 mL of solution in a  
153 tube for ICP-MS analyses.

154 The dissolved fraction was analysed by IC (IC 850 Metrohm) for the inorganic and organic anions

Commented [RS(-S11)]: At the point when it would have been deposited to the surface ocean.

Commented [RS(-S12)]: No need to define as you don't use this abbreviation elsewhere

Formatted: Strikethrough

Commented [RS(-S13)]: The

Commented [RS(-S14)]: This should be number 1 as it is the focus of the paper. List = i) TMs, ii) DOC, iii) major seawater and atmospheric ions, iv) pH. Then a description of the methods used for each, in the order they are listed



155 (NO<sub>2</sub>, NO<sub>3</sub>, PO<sub>4</sub><sup>3-</sup>, SO<sub>4</sub><sup>2-</sup>, F, Cl, Br, HCOO<sup>-</sup>, CH<sub>3</sub>COO<sup>-</sup>, C<sub>2</sub>H<sub>5</sub>COO<sup>-</sup>, MSA, C<sub>2</sub>O<sub>4</sub><sup>2-</sup>) and for the cation  
156 NH<sub>4</sub><sup>+</sup> (Mallet et al., 2017). ~~On the other hand,~~ the dissolved fraction and solution from ~~the~~ digestion  
157 of ~~the~~ particulate fraction ~~of the rain samples~~ were analysed by ICP-AES (Inductively Coupled  
158 Plasma Atomic Emission Spectrometry, Spectro ARCOS Ametek®) for major elements (Al, Ca, K,  
159 Mg, Na, S) (Desboeufs et al., 2014) and by HR-ICP-MS (High Resolution Inductively Coupled Plasma  
160 Mass  
161 Spectrometry, Neptune Plus™ at Thermo Scientific™) for TMs: Cd, Co, Cr, Cu, Fe, Mn, Mo, Ni, P,  
162 Pb, Ti, V and Zn. The speciation of dissolved P was estimated by determining ~~the~~ dissolved inorganic  
163 phosphorus (DIP) from phosphate concentrations expressed as P and the dissolved organic phosphorus  
164 (DOP) from the difference between total dissolved phosphorus (TDP), obtained by ICP-MS, and DIP,  
165 obtained by IC.

Commented [RS(-S15)]: You don't present this data here – note this

Commented [RS(-S16)]: Move up to where the rest of the ICP stuff is

166 In order to estimate the contamination of sampling and analytical protocols, ~~3~~ three blanks of rain  
167 samples (collected on-board during the cruise with the same protocol without rain events) were used  
168 and processed. The procedural limit of detections (LoD) were defined as 3 x standard deviation of  
169 blank samples both for dissolved and particulate fractions estimated after acid digestion. All ~~samples~~  
170 dissolved and particulate ~~sample~~ concentrations were higher than LoD, except for NO<sub>2</sub> in the two rain  
171 samples. The blank concentrations represented 10.2% ~~on~~ average for TMs and were typically lower  
172 than 20% of the sample concentrations, except for Cd (52%) and Mo (43%) in the dissolved fraction.  
173 ~~For the sample concentration computations, we subtracted these blanks values to elemental~~  
174 ~~concentrations obtained in rain samples. Blank concentrations were subtracted from all sample~~  
175 ~~concentrations.~~

Commented [RS(-S17)]: More detail needed. Not clear what the rain blanks were. What were the blanks for the dissolved fraction? Empty bottles swished out with MQ or acidified MQ and a filter? Blanks and LoDs can be found where?

Formatted: Strikethrough

## 176 2.2 Atmospheric ancillary measurements

177  
178 The PEGASUS (PortaBLE Gas and Aerosol Sampling UnitS, [www.pegasus.cnrs.fr](http://www.pegasus.cnrs.fr)) mobile platform  
179 of LISA is a self-contained facility based on two standard 20-foot containers, adapted with air  
180 conditioning, rectified power, air intake and exhausts for sampling and online measurements of  
181 atmospheric aerosols and gaseous compounds, and their analysis (Formenti et al., 2019). During the  
182 PEACETIME cruise, only the sampling module of the facility was deployed on the starboard side of  
183 deck 7 of the R/V. The PEGASUS instrumental payload of relevance to this paper included  
184 measurements of the major gases such as NO<sub>x</sub>, SO<sub>2</sub>, O<sub>3</sub> and CO by online analysers (Horiba APNA,  
185 APSA, APOA and PICARRO respectively; 2-min resolution, detection limit ~~for all analytes was~~ 0.5  
186 ppb and 1 ppb for CO). ~~These gases, that~~ were used to estimate ~~the~~ origins of ~~collected air masses~~  
187 ~~sampled air~~.  
188 From ~~the first of~~ 1st June 2017 (?) (not operational before), additional measurements by an ALS450®  
189 Rayleigh-



190 Mie lidar (Leosphere™; Royer et al., 2011) ~~was~~were used to monitor the vertical distribution of  
191 aerosols over time and the associated integrated columns. The vertical lidar profiles were analysed to  
192 yield the apparent backscatter coefficient (ABC) corrected from the molecular transmission, as well  
193 as the volume depolarisation ratio (VDR). The inversion procedure (Chazette et al., 2016; 2019) to  
194 retrieve the aerosol extinction coefficient (unit km<sup>-1</sup>) uses a vertical-dependent lidar ratio that takes  
195 into account two aerosol layers. The first layer corresponds to marine aerosols in the marine boundary  
196 layer (MBL), the second to a desert aerosol layer that can extend between ~1 and 6 km above mean  
197 sea level (amsl). In accordance with Chazette et al. (2016), for the same wavelength and region, the  
198 lidar ratios were set to 25 and 55 sr, respectively. The vertical profile of the aerosol extinction  
199 coefficient was retrieved from 0.2 km amsl ~~on~~upwards with a vertical resolution of 15 m. Based on  
200 these profiles, the integrated column content of dust aerosols was estimated using a specific extinction  
201 cross-section of 1.1 m<sup>2</sup> g<sup>-1</sup> as proposed by Raut and Chazette (2009).

202 In addition, detailed meteorological data such as air and sea temperature, atmospheric pressure,  
203 relative humidity, atmospheric pressure, heat flux and wind speed and direction were provided on a  
204 30 seconds ~~time~~step basis by the ship's permanent instrumentation.

### 205 2.3 Sampling and analysis of dissolved TMs in seawater

206 Before and after each rain, seawater samples were collected in the surface microlayer (SML: <1 mm)  
207 and subsurface seawater (SSW: <1 ~~m~~m depth) (Tovar-Sánchez et al., 2020, this ~~special~~issue). SML  
208 and SSW samples were collected from a pneumatic boat 0.5-1 nautical miles ~~away~~away from the R/V in  
209 order to avoid any potential contamination. SML samples were collected using a silicate glass plate  
210 sampler (Stortini et al., 2012; Tovar-Sánchez et al., 2019) which had previously been acid-cleaned  
211 ~~with acid~~overnight and rinsed thoroughly with ultrapure water (~~MQ-water~~18 mΩ cm<sup>-1</sup>). The 39 x 25  
212 cm ~~silicate~~glass plate had an effective sampling surface area of 1950 cm<sup>2</sup> considering both sides. In  
213 order to check for procedural contamination, SML blanks were collected at some stations on board of  
214 the pneumatic boat by rinsing the glass plate with ultra-pure water and collecting 0.5 L of ultra-pure  
215 water using the glass plate system. The surface microlayer thickness was calculated following the  
216 formula of Wurl (2009). SSW was collected by using ~~an~~acid-washed Teflon tubing connected to a  
217 peristaltic pump. The total fraction (i.e. T-SML) was directly collected from the glass plate system  
218 without filtration into ~~a~~0.5 L acid cleaned LDPE bottles, while the dissolved fraction in the SML (i.e.  
219 D-SML) and SSW (i.e. D-SSW) was filtered in situ through an acid-cleaned polypropylene cartridge  
220 filter (0.22 µm; MSI, Calyx®).

221 TMs samples were also collected in the water column using ~~the a~~titanium trace metal~~s~~ clean (TMC)  
222 rosette (mounted with 24 teflon-coated Go-Flo bottles) before and after the rain events (Bressac et  
223 al., 2021). Although rosette deployments were performed over the whole water column, we focus here

**Commented [RS(-S18):** By rinsing the glass plate with 0.5 L of ultra-pure water; this water was collected as the blank solution?

**Formatted:** Font: Italic



224 on the 0-20 m ~~marine~~-mixed-layer (ML). ~~The water column was sampled using the TMC titanium~~  
225 ~~rosette mounted with 24 teflon-coated Go-Flo bottles.~~

226 Immediately after recovery, the Go-Flo bottles were transferred inside a class-100 clean laboratory  
227 container. Seawater samples were directly filtered from the bottles through acid-cleaned 0.2- $\mu$ m  
228 capsule filters (Sartorius Sartobran-P-capsule 0.45/0.2- $\mu$ m). All samples were acidified on board to  
229 pH < 2 with Ultrapure-grade HCl under a class-100 HEPA laminar flow hood. Metals (namely Cd,  
230 Co, Cu, Ni, Mo, V, Zn and Pb) were pre-concentrated using an organic extraction method (Bruland et  
231 al., 1979) and quantified by ICP-MS (Perkin Elmer ELAN DRC-e) ~~in the home laboratory~~. In order  
232 to breakdown metal-organic complexes and remove organic matter (Achterberg et al., 2001; Milne et  
233 al., 2010), ~~the total fraction samples~~ (i.e. T-SML) were ~~digested-UV-treated~~ prior to the pre-  
234 concentration ~~step~~ using a UV system consisting of one UV (80 W) mercury lamp that irradiated the  
235 samples (contained in quartz bottles) ~~during for~~ 30 min. The accuracy of the pre-concentration method  
236 and analysis for TMs was established using Seawater Reference Material (CASS 6, NRC-CNRC) with  
237 recoveries ranging from 89% for Mo to 108% for Pb. Due to the complexity of the analytical method,  
238 all the TMC samplings were not analysed for ~~these metals~~. Overall, 1 or 2 depths were obtained in the  
239 mixed layer (0-20 m). Dissolved Fe and Al concentrations were also measured on board. Dissolved  
240 Fe concentrations were measured using an automated Flow Injection Analysis (FIA) with online  
241 pre-concentration and chemiluminescence detection (Bonnet and Guieu, 2006), and dissolved Al  
242 concentrations using the fluorometric method described by Hydes and Liss (1976). Sampling and  
243 analysis for dissolved Fe and Al concentrations are fully described in Bressac et al. (2021), and  
244 covered at least ~~4-four~~ depths in the 0-20 m mixed layer.

#### 245 2.4 Enrichment factor and solubility

246 In order to better constrain the origin of TMs in the rain samples, their enrichment factor  $\epsilon$ (EF; Rahn  
247 1976) relative to the Earth's crust ~~was were~~ calculated based on their total concentrations (dissolved  
248 + particulate fractions) as:

$$249 \quad EF = \frac{([X]/[Al])_{sample}}{([X]/[Al])_{crust}} \quad (1)$$

250 where  $[X]/[Al]$  is the ratio between an element X and Al concentrations in rainwater samples (at the  
251 numerator), and in the Earth's crust (denominator) from Rudnick and Gao (2003). Aluminium is  
252 currently used as a reference element as it ~~only has a crustal origin~~. For a given TM,  $EF > 1$  indicates  
253 an enrichment with respect to the average composition of the Earth's crust. To account for the soil  
254 composition variability of mineral dust ~~atmospheric~~-sources, TMs with an EF value  $> 10$  are  
255 considered ~~significantly enriched, which points to a derived from~~-non-crustal sources (Rahn, 1976).

256 The relative solubility of TMs in the two rainwater events was calculated as:

Commented [RS(-S19)]: Which metals? Mo and Pb or not all samples were pre-concentrated for all metals listed?

Commented [RS(-S20)]: Not exactly but the vast majority of Al is crustal. Therefore, it is currently accepted as one of the best proxy elements. It is predominantly crustal



257 
$$S_X\% = \frac{[X]_{\text{dissolved}}}{[X]_{\text{total}}} \times 100 \quad (2)$$

258 where  $S_X\%$  is the relative solubility (in %) of an element X in the rainwater,  $[X]_{\text{dissolved}}$  and  $[X]_{\text{total}}$  are  
259 its soluble and total concentration, respectively.

## 260 2.5 Atmospheric deposition fluxes

261 Impacts on biogeochemical cycles and ecosystem functioning after a rain event occur on time scales  
262 of a few days (2-3), and space scales of tens of km (about 20-50 km within the radius of the ship's  
263 position). In the specific context of oceanographic cruising, the documentation of these impacts is  
264 restricted to the vertical dimension at the prescribed temporal scale. In this vertical dimension, the  
265 exchange of TMs ~~aeross-into~~ the ML was controlled both by atmospheric inputs over the R/V position  
266 and by advection from surrounding water masses that may have been impacted by surrounding  
267 rainfall. Therefore, we had to consider this process in our estimation of the atmospheric fluxes  
268 contributions. For this purpose, the atmospheric fluxes have to be integrated to the extent of the rain  
269 area that can impact the marine surface layers. We derived wet deposition fluxes by considering the  
270 total precipitation accumulated during the duration of the rain over the area around the R/V location.  
271 Thus, the wet deposition fluxes in our rain samples were calculated by multiplying the volume  
272 weighted mean rainfall concentration by the total precipitation ([equation and explanation for using  
273 VWM rainfall here](#)). The total precipitation of the rain events was issued from the hourly total  
274 precipitation accumulated during the rain events over the region from ERA5 ECMWF reanalysis  
275 (Herbasch et al., 2018) and from the rain rate composite radar products from the European OPERA  
276 database (Saltikoff et al., 2019), when it ~~was~~ possible. Although subject to uncertainties (Morin et al.,  
277 2003), a surface-based weather radar is probably the best tool to estimate rainfall in the surroundings  
278 of the R/V ~~because...~~. However, the OPERA database does not include Italian radars, which ~~anyway~~  
279 did not cover the central area of the Ionian Sea during the cruise ~~anyway~~. ERA5 data are available on  
280 regular latitude-longitude grids at 0.25° x 0.25° resolution. The accumulated precipitation was taken  
281 from the grid-points spanning the ship's location, ~~more or less approximately~~ 0.25° around the central  
282 grid-point for integrating the regional variability. Surface rain rate radar composite images were  
283 available every 15 minutes with a spatial resolution of 2 km x 2 km. The accumulated precipitation  
284 was the sum of ~~integrared (?)~~ rain rates during the rain duration averaged over the radar pixels  
285 spanning the ship's location within a radius of about 25 km around the ship location.

## 286 2.6 Stocks in the surface seawater

287 For the surface microlayer (SML), stocks of TMs were estimated from the integration of TM  
288 concentration over the thickness of the ~~layer~~SML. The thickness ranged from 32 µm and from  
289 26 to 43 µm at ION and FAST, respectively (Tovar-Sanchez et al., 2020).

Commented [RS(-S21)]: Sometimes ship, sometimes R/V, perhaps best to stick with one



290 The trace metals stocks within the ML were calculated by trapezoidal integrations of marine  
291 concentrations from SSW and TMC rosette samplings. The upper water column was stratified along  
292 the cruise transect (Taillandier et al., 2020), with a ML depth ranging from 7 to 21 m (11 to 21 m at  
293 ION station and 11 to 19 m at FAST station (Van Wambeke et al., 2020). The ML depth (MLD)  
294 fluctuations, ~~for example~~ due to wind peaks associated with rain events for example, could create  
295 rapidly changing conditions of vertical advection from deeper waters. However, with no significant  
296 increase in TMs concentrations being observed below the ML down to about 50 m (not shown), the  
297 enrichment observed in the ML after rainfalls could not be attributed to any mixing with deeper water  
298 due to high wind. In consequence, stocks in the ML have been integrated over a constant depth range  
299 of 0-20 m for comparison, ~~as in accord with~~ Bressac et al. (2021). For Cu, Fe, Ni ~~and~~ Zn, stocks were  
300 estimated both for the dissolved and particulate fractions in the SML and ML, for Co, Cd, Mo, Pb and  
301 V for the dissolved fraction only in the ML and for both fractions in the SML and for Mn and Ti only  
302 for the particulate fraction in the ML.

Commented [RS(-S22)]: ML, ML depth or MLD - consistency

303 The partitioning coefficient between the particulate and dissolved phases ( $K_d$   
304 = [particulate]/[dissolved]) was used to investigate exchanges between the dissolved and particulate  
305 pools of TMs (ref).

Commented [RS(-S23)]: Why was this? Because of concs below the LoD?

### 306 3. Results

#### 307 3.1 General conditions

308 The general meteorological conditions during the cruise indicated that the ION and FAST stations  
309 were highly affected by cloudy weather conditions. During these periods, ~~2-two~~ significant rain  
310 ~~events~~ occurred ~~over~~ the R/V's position and ~~have been collected~~ were sampled. The first rain  
311 ~~sample~~ (hereafter Rain ION) was collected during the 4-day ION station occupation in the Ionian Sea  
312 in the early morning of 29/05 at 03:08  
313 UTC, ~~and~~ the second rain event (hereafter Rain FAST) occurred during the 5-day "Fast action"  
314 station, (hereafter FAST) in the Algerian Basin during the night of 05/06 at 00:36 UTC (Table 1).  
315 The two rain sample ~~collections~~ coincided with peaks in relative humidity and wind speed, and  
316 minima in air temperature (not shown).

Commented [RS(-S24)]: 09/05/2017. Date here is numeric, earlier it is longhand 1<sup>st</sup> September

Commented [RS(-S25)]: Unnecessary – you've been referring to them already

317 Table 1: Information regarding the two rains collected during the PEACETIME cruise.

Sample	Sampling time	Station name (dates) and rain location	Estimated total precipitation
Rain ION	29 May 2017, 03:08-04:00 (UTC) 05:08-06:00 (local time)	ION (25-29 May) 35.36°N, 19.92°E	3.5 ± 1.2 mm



Rain FAST	05 June 2017, 00:36-01:04 (UTC) 02:36-03:04 (local time)	FAST (2-7 June) 37.94°N, 2.91°E	6.0 ±1.5 mm
-----------	--	------------------------------------	-------------

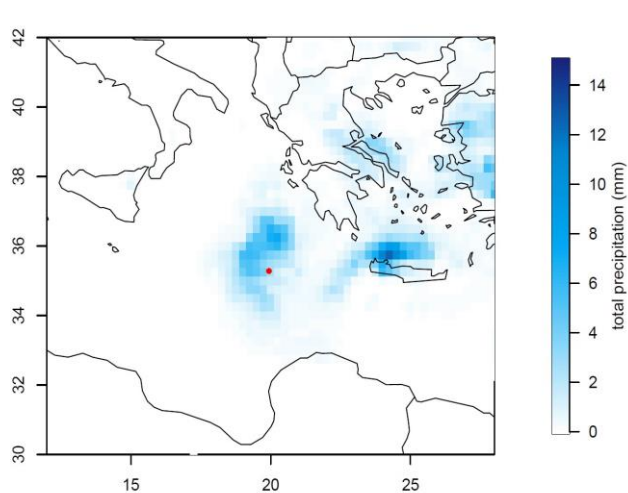
318

319 *3.1.1. Rain ION*

320 The ERA 5 data reanalysis shows ~~2~~two periods of precipitation in the ~~surrounding-of~~vicinity of the  
321 ship's position, i.e. in the morning and evening of June 26 (not shown) and in the night between June  
322 28 and 29, in agreement with on-board visual observations. The rain event collected at ION was the  
323 product of a large cloud system, covering an area of about 90 000 km<sup>2</sup> around the R/V position,  
324 spreading over the Ionian and Aegean Seas (Fig. 1). ~~As n~~No radar measurements ~~being-were~~ available  
325 for this area, the accumulated rate (~~3.5 ±1.2 mm~~) was estimated from ERA 5 data reanalysis on the  
326 grid-point corresponding to the ION station ~~and was 3.5 ±1.2 mm(±0.25°)~~-around the R/V position  
327 (~~±0.25°~~). The wash-out of the atmospheric particles was revealed by the decrease in aerosol number  
328 concentrations monitored onboard from about 1900 to 300 part.cm<sup>-3</sup> (supplementary material Fig. S1).  
329 Air mass back-trajectories showed that the scavenged air masses came from Greece both in the marine  
330 boundary layer and in the free troposphere (Fig. S1). The satellite observations ~~also~~ showed low  
331 aerosol optical thickness during this period (not shown), meaning low amounts of aerosols in the  
332 atmospheric column. No significant European pollution influence was monitored by ~~on-board~~  
333 measurements during this event, with major gas mixing ratios and aerosol concentrations ~~in-close to~~  
334 the average values of the cruise (Fig. S1) and typical of clean atmospheric concentrations, i.e. under  
335 detection limit for NO<sub>x</sub>, 1.2 ppb for SO<sub>2</sub>, 51 ppb for O<sub>3</sub>, 80 ppb for CO and 3000 part.cm<sup>-3</sup>. On this  
336 basis, this wet event was representative of a Mediterranean background marine rain event. (~~ref for~~  
337 ~~these typical background concs~~).

Commented [RS(-S26)]: Rate requires a time dimension

Commented [RS(-S27)]: Onboard is one word – several cases need correcting



Commented [RS(-S28)]: It would be nice to have S3 in this figure for comparison instead of in the SI

338

339 **Figure 1: Total precipitation (mm) between 28 May 2017 at 20:00 UTC and 29 May 2017 at 10:00**  
340 **UTC from ERA5 ECMWF reanalysis. The red circle indicates the R/V position.**

### 341 3.1.2. Rain FAST

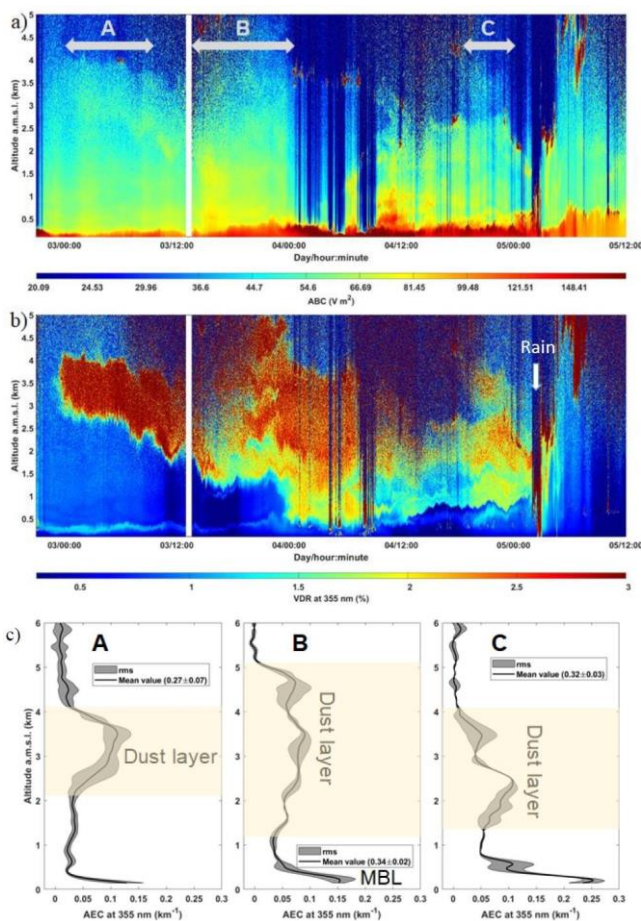
342 As detailed in Guieu et al. (2020), the FAST station position was decided on the basis of regional  
343 model forecast runs and satellite observations, ~~in~~ for the purpose ~~to~~ of catching a wet dust deposition  
344 event. Significant dust emissions were observed from NASCube (<http://nascube.univ-lille1.fr/>,  
345 Gonzales and Briottet, 2017) over North Africa from the night of 30-31 May, then new dust emissions  
346 in the night from 3 to 4 June in Algeria and southern Morocco associated with a northward atmospheric  
347 flux. On 30 May, the SEVIRI AOD satellite product ([https://www.icare.univ-](https://www.icare.univ-lille.fr/dataaccess/browse-images/geostationary-satellites/)  
348 [lille.fr/dataaccess/browse-images/geostationary-satellites/](https://www.icare.univ-lille.fr/dataaccess/browse-images/geostationary-satellites/), Thieuleux et al., 2005) confirmed the  
349 presence of atmospheric dust in a cloudy air mass over the western part of the Mediterranean, and  
350 from 2 June the export of a dust plume from North Africa south of the Balearic Islands with high  
351 AOD (>0.8) on the Alboran Sea was observed (Fig. S2). The dust plume was transported to the NE  
352 up to Sardinia on June 4, with AOD <0.5 ~~in all the area and e~~. Clear sky with low AOD was ~~left~~  
353 ~~observed~~ west of 4°E on June

354 5.

355 On-board lidar measurements (Fig. 2 a,b,c) showed that the aerosol plume was present over the ship's  
356 position from 2 June at 21:00 UTC until the rain event, and corresponded to a dust aerosol layer ~~well~~  
357 highlighted by the high depolarization. The dust plume was concentrated between 3 and 4 km at the  
358 beginning of the station occupation, then expanded down to the marine boundary layer (about 500 m



359 ~~amsl) by~~ the end of the day on 3 June 2017 ~~3~~ down to the marine boundary layer (about 500 m amsl).  
 360 The mass integrated ~~contents-concentration~~ of dust aerosols derived from the profiles of aerosol  
 361 extinction ranged from a minimum of  $0.18 \pm 0.005 \text{ g m}^{-2}$  just before the rain to a maximum of  $0.24$   
 362  $\pm 0.009 \text{ g m}^{-2}$ , where standard deviations indicate the temporal variability (1 sigma).



363  
 364 **Figure 2:** On-board lidar-derived a) Apparent backscatter coefficient (ABC), (b) Temporal evolution  
 365 (in Local-local Time) of the lidar-derived volume depolarization ratio (VDR) where the dust  
 366 plume is highlighted for values higher than ~1.7 (yellow to red colours) and the rain by values higher  
 367 than 3 (indicated by the arrow), and c) vertical profiles of the aerosol extinction coefficient (AEC) in  
 368 cloud free condition, integrated over 3 periods along the dust plume event, noted A, B and C in

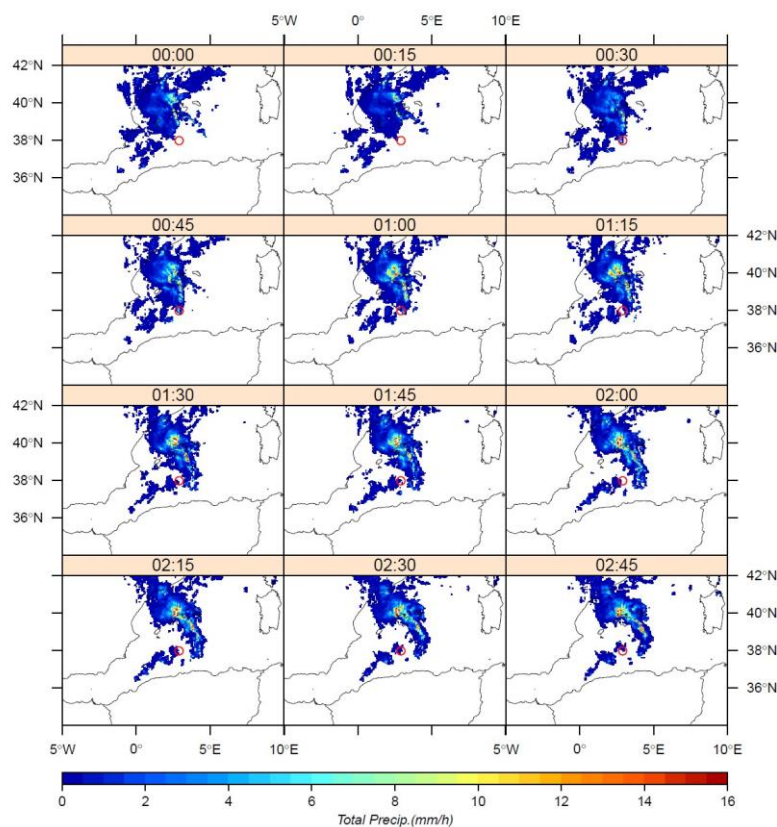
**Commented [RS(-S29)]:** Can these panels be relabelled?  
 You have panels a-c and labelling within panel a of arrows a-  
 c, and in panel c of box a-c. All these a-cs get a bit confusing



369 ~~panel figure a (top)~~. The grey shade represents the root mean square (rms) variability along the time  
370 of the measurement. The dust layer is highlighted on the profiles. The mean aerosol optical thickness  
371 is given in the boxed legend with its temporal variability (1 sigma). The location of the marine  
372 boundary layer (MBL) is also pointed.

373 Rainfalls were ~~was~~ observed by weather radar images in the ~~neighbouring~~ area of the R/V  
374 ~~neighbouring~~ from 3 June at 7:00 UTC. The rainfalls recorded around the FAST station ~~were was~~  
375 associated with ~~2-two~~ periods of rain: ~~the 03/06~~ from 07:00 to 14:00 UTC ~~on 03/06~~, and from ~~the~~  
376 ~~04/06 at 16:00 UTC on 04/06~~ to ~~05/06 at 06:00 UTC on 05/06~~. For this latter ~~case~~, a rain front (100  
377 000 km<sup>2</sup>), moving eastward from Spain and North Africa regions, reached the FAST station the night  
378 between the 4 and 5 June (Fig. 3). Wet deposition between the 4 and early 5 June in the FAST station  
379 area were confirmed by radar imagery, showing several other ~~instances of rain spots~~ around the R/V  
380 position before and after the rain sampling (Fig. 3). Continuous on-board lidar measurements  
381 confirmed the below-cloud deposition during the rain event of early 5 June (Fig. 2b). Rain FAST was  
382 a wet deposition event occurring at the end of an episode of transport of Saharan dust, whereas  
383 precipitation ~~of on~~ the 3 June occurred during the maximum of the dust plume (Fig. 2b and S2). The  
384 surface concentrations of gas and particles, measured on-board, suggest no clear dust or anthropogenic  
385 influence in the atmospheric boundary layer during ~~the this~~ period of wet deposition, in agreement  
386 with back trajectories of low altitude air masses (Fig S2.), presuming no local mixing between dust  
387 and anthropogenic particles into rain samples. The total precipitation estimated from radar rainfall  
388 ~~estimates~~ yield an accumulated precipitation of  $6.0 \pm 1.5$  mm ( $\pm 25$  km around ~~the ship's position~~), in  
389 agreement with ECMWF reanalysis ERA5 (Fig. S2) for the wet deposition on the night of 4-5 June  
390 ( $5.7 \pm 1.4$  mm in the grid-point spanning the R/V position, i.e.  $\pm 0.25^\circ$  ~~around~~).

Commented [RS(-S30): repetition



391

392 **Figure 3:** Rain rates (mm/h) during the night between the 4 and 5 June, when Rain ~~Fast-FAST~~ was  
393 ~~been~~ collected on-board, issued from European rain radar composites (OPERA programme) of ~~5~~  
394 ~~June 5~~ between 00:00 and 02:45 UTC.

### 395 3.2. Chemical composition of rains

396 Dissolved and total concentrations of nutrients and TMs in the rain samples are presented in Table 2.  
397 Among all measured dissolved concentrations,  $\text{NO}_3^-$  was the most abundant nutrient, followed by  
398 ammonium (Table 2). The nitrite concentration was ~~under-below~~ the limit of detection for the two rain  
399 samples. Regarding TMs in rain, Fe and Zn presented the highest concentrations in rain samples with  
400 the same order of magnitude (10 to 25  $\mu\text{g L}^{-1}$ ). Co, Cd and Mo had the lowest concentrations

Commented [RS(-S31)]: Use ionic formula or name, not both in the same sentence

380 (<0.1 µg L<sup>-1</sup> in both events), whereas the other TMs concentrations ranged

between 0.1 and 10 µg 381 L<sup>-1</sup> in both rain samples (Table 2). Concentrations of nutrients and the majority of TMs were higher in the 382 dust-rich rain, except for Pb (similar concentrations in both rain samples) and Cr (3 times higher concentration 383 in Rain ION relative to Rain FAST).

384 Table 2: Dissolved and total concentrations of nutrients and TMs in the two rain samples collected during the 385 PEACETIME cruise in µg.L<sup>-1</sup> or ng.L<sup>-1</sup> and µmol.L<sup>-1</sup> or nmol.L<sup>-1</sup> in the parentheses (sd = standard deviation 386 from three replicates).

		Rain ION				Rain FAST				
		Dissolved		Total		Dissolved		Total		
		concentrations	±sd	concentrations	±sd	concentrations	±sd	concentrations	±sd	
<b>Nutrients</b>	NO <sub>3</sub> <sup>-</sup>	µg L <sup>-1</sup> (µmol L <sup>-1</sup> )	1185 (19.1)	71 (1.1)			3694 (59.6)	222 (3.6)		
	NH <sub>4</sub> <sup>+</sup>	µg L <sup>-1</sup> (µmol L <sup>-1</sup> )	366 (20.3)	11 (0.6)			654 (36.3)	19 (1.1)		
	DIN	µg L <sup>-1</sup> (µmol L <sup>-1</sup> )	552 (39.4)	82 (1.7)			1343 (96)	241 (1.7)		
	PO <sub>4</sub> <sup>3-</sup>	µg L <sup>-1</sup> (nmol L <sup>-1</sup> )	18.1 (189)	0.5 (6)			19.0 (200)	0.6 (6)		
	DIP	µg L <sup>-1</sup> (nmol L <sup>-1</sup> )	5.87 (189)	0.18 (6)			6.20 (200)	0.19 (6)		
	DOP	µg L <sup>-1</sup> (nmol L <sup>-1</sup> )	8.63 (278)	1.94 (75)			4.91 (158)	1.56 (57)		
	TP	µg L <sup>-1</sup> (nmol L <sup>-1</sup> )	14.51 (468)	2.52 (81)	16.6 (536)	1.0 (33)	11.11 (358)	1.95 (63)	58.7 (1894)	3.5
	DIN/DIP		(208)				(480)			
	DOC	(µmol L <sup>-1</sup> )	(105.7)	(2.2)			(95.5)	(1.2)		
	<b>Metals</b>	Al	µg L <sup>-1</sup> (nmol L <sup>-1</sup> )	13.0 (480)	0.5 (30)	14.6 (540)	0.9 (32)	23.4 (867)	0.7 (24)	440 (16308)
Cu		µg L <sup>-1</sup> (nmol L <sup>-1</sup> )	0.71 (11.1)	0.02 (0.3)	0.73 (11.5)	0.02 (0.3)	1.15 (18.0)	0.04 (0.6)	1.63 (25.7)	0.06
Fe		µg L <sup>-1</sup> (nmol L <sup>-1</sup> )	15.1 (270)	0.4 (6)	17.9 (321)	0.6 (11)	19.2 (344)	0.1 (2)	231 (4140)	7
Mn		µg L <sup>-1</sup> (nmol L <sup>-1</sup> )	0.55 (10.0)	0.02 (0.3)	0.60 (10.9)	0.02 (0.4)	3.17 (57.8)	0.07 (1.2)	5.26 (95.7)	0.12
Ni		µg L <sup>-1</sup> (nmol L <sup>-1</sup> )	0.52 (8.8)	0.02 (0.3)	0.67 (11.4)	0.02 (0.4)	0.59 (10.1)	0.02 (0.4)	0.84 (14.3)	0.03
Ti		µg L <sup>-1</sup> (nmol L <sup>-1</sup> )	0.48 (10.0)	0.04 (0.8)	0.65 (13.6)	0.48 (3.2)	0.22 (4.7)	0.01 (0.1)	33.36 (697)	0.51
V		µg L <sup>-1</sup> (nmol L <sup>-1</sup> )	0.37 (7.4)	0.01 (0.2)	0.38 (7.42)	0.01 (0.25)	1.37 (26.9)	0.03 (0.5)	2.02 (39.7)	0.04
Zn		µg L <sup>-1</sup> (nmol L <sup>-1</sup> )	24.8 (379)	0.8 (12)	25.3 (387)	0.8 (12)	22.7 (347)	0.6 (8)	26.3 (402)	0.7
Cd		ng L <sup>-1</sup> (pmol L <sup>-1</sup> )	12.9 (115)	6.4 (57)	13.1 (117)	6.3 (56)	20.2 (180)	10.3 (92)	23.7 (210)	6.8
Co		ng L <sup>-1</sup> (pmol L <sup>-1</sup> )	44 (749)	13 (229)	47.4 (804)	14.5 (246)	82 (1386)	20 (347)	157 (2661)	28
Cr		ng L <sup>-1</sup> (pmol L <sup>-1</sup> )	241 (4636)	16 (300)	628 (12079)	5 (95)	79 (1522)	14 (260)	443 (8514)	43
Mo		ng L <sup>-1</sup> (pmol L <sup>-1</sup> )	28 (288)	10 (106)	4.1 (43)	1.4 (14)	82 (855)	11 (113)	92.1 (960)	16.2
Pb		ng L <sup>-1</sup> (pmol L <sup>-1</sup> )	170 (822)	11 (54)	175.1 (845)	1.4 (7)	166 (801)	9 (41)	604 (2917)	19

387

### 388 3.3. Marine concentrations and stocks

389 All the TMs had significantly higher concentrations in the ML compared to deep water masses, in  
 390 agreement with a stratified profile associated with atmospheric input. The particulate and dissolved  
 391 trace metal concentrations within the ML (0-20 m) and the SML are displayed in Fig. 4.392  
 Concentrations were of the same order of magnitude in-at the two studied stations ION and FAST, except for  
 the 393 particulate phase in the SML where the concentrations of Cu and Co were significantly lower (values)  
 at 394 ION station. The TMs were mainly in dissolved forms in the ML (range of values), except for Fe,  
 whose dissolved 395 and particulate concentrations were on the same order of magnitude (values). On the  
 contrary, the particulate 396 phase contribution dominated for TMs in the SML, in particular at the ION  
 station. At both stations, 397 the highest TMs concentrations in the surface seawater were found for Mo in  
 the dissolved fraction (values).

Commented [RS(-S32)]: Are you really talking about deep water masses or just the water below the ML?

Formatted: Indent: First line: 0 cm

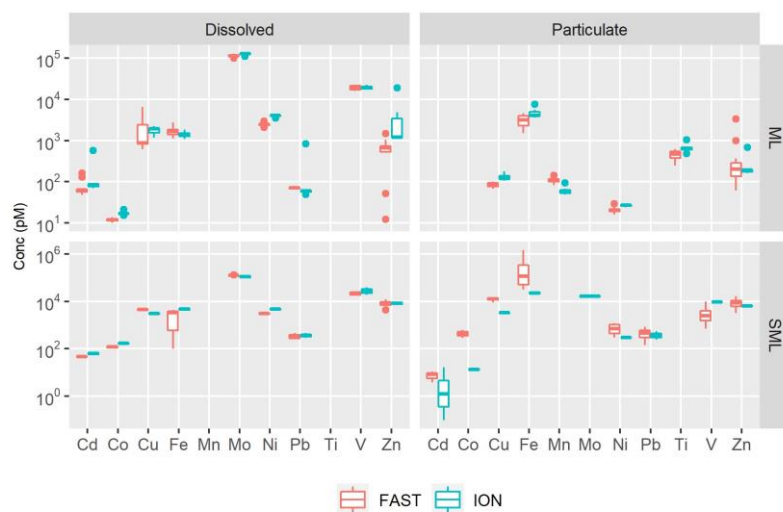


397 in agreement with the abundance of dissolved Mo in seawater (~ 107 nM, Smedley and Kinniburgh,  
398 2017), and Fe in the particulate fraction (value). All the particulate and dissolved TMs concentrations  
399 measured during the cruise were representative within the range previously published for the  
400 Mediterranean Sea (Sherrell and Boyle, 1988; Saager et al., 1993; Morley et al., 1997; Yoon et al.,  
401 1999; Wuttig et al., 2013; Baconnais et al., 2019; Migon et al., 2020). Zn presented the largest range  
402 of concentrations within the ML both in the particulate and dissolved phases (values), due to some  
403 high concentrations. However, the concentrations stayed in the typical range of values found reported  
404 in for the Mediterranean Sea (Bethoux et al., 1990, Yoon et al., 1999). The concentrations in in the  
405 SML, the concentrations were lower than in the ML and Pb dominated both in dissolved and  
406 particulate phases. Tovar-Sanchez et al. (2020) showed that the TMs concentrations in the SML during  
407 the PEACETIME campaign were generally lower than those previously measured in the  
408 Mediterranean Sea, except in for the particulate phase during at the FAST station after following  
409 dust deposition.

Commented [RS(-S33)]: Did any of these studies determine pMo and/or dMo? If not, say that yours are the first

Commented [RS(-S34)]: Was contamination suspected?

Commented [RS(-S35)]: I don't understand this statement



410

411 **Figure 4:** Box plots of dissolved (left panels) and particulate (right panels) marine concentrations  
412 (pM) for the different TMs within the ML (upper panels) and the SML (lower panels) at ION (green)  
413 and FAST (red) stations. In the box plots, the box indicates the interquartile range, i.e. the 25th and  
414 the 75th percentile, and the line within the box marks the median. The whiskers indicate the quartiles

Commented [RS(-S36)]: Could these be plotted on the same scale to make it easier to compare the SML and ML concs?



415  $\pm 1.5$  times the interquartile range. Points above and below the whiskers indicate outliers outside the  
416 10-th and 90th percentile.

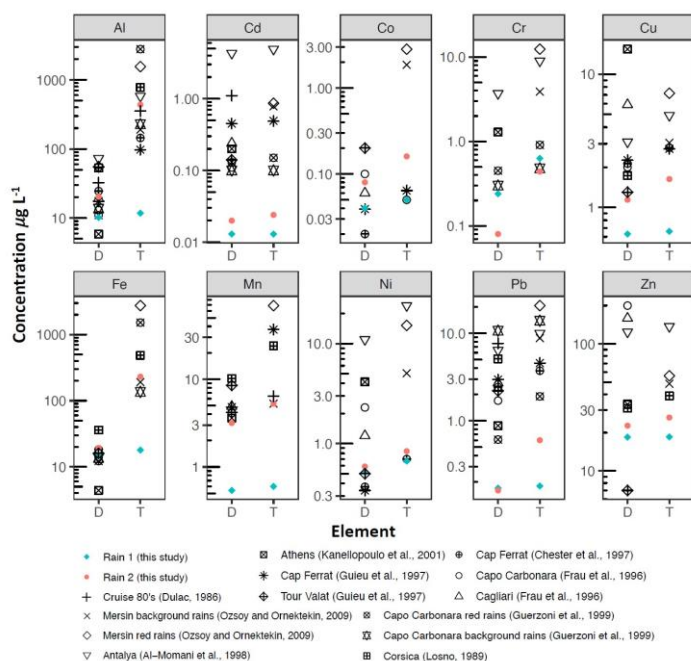
#### 417 4. Discussion

##### 418 4.1. Composition of rain collected over the remote Mediterranean Sea

###### 419 4.1.1. Concentrations

420 Regarding nutrients, nitrogen species concentrations in rain samples were in good agreement with  
421 those reported in Mediterranean rain samples, ranging from 1130 to 5100  $\mu\text{g L}^{-1}$  for  $\text{NO}_3^-$  and between  
422 207 and 1200  $\mu\text{g L}^{-1}$  for  $\text{NH}_4^+$  (Loye-Pilot et al., 1990; Avila et al., 1997; Al Momani et al., 1998;  
423 Herut et al., 1999; Violaki et al., 2010; Izquieta-Rojano et al., 2016; Nehir and Koçak, 2018). The  
424 FAST rain concentrations were within the average values published range, whereas the ION rain was  
425 in the low range, confirming a background signature at this station. The rainwater samples presented  
426 a large dominance of N in comparison to P, as observed from the N/P ratio derived from DIN/DIP  
427 (Table 2) ranging from 208 at ION to 480 at FAST. Previous observations showed a predominance of  
428 N relative to P in ~~the~~ atmospheric bulk deposition over the Mediterranean coast, with ratios higher  
429 than the Redfield ratio (Markaki et al., 2010, Desboeufs et al., 2018). The highest ratio observed  
430 reached 1200 (in the case of DIN/TDP), but ~~were on average~~ around about 100 in bulk deposition  
431 (unfiltered rain). The highest ratio could be linked to a washout effect of ~~the~~ gaseous N species (as  
432  $\text{NO}_x$  and  $\text{NH}_3$ ) by rain (Ochoa-Hueso et al., 2011). At the two stations, no high  $\text{NO}_x$  concentrations  
433 were observed in the boundary layer before wet deposition (range). The presence of nitrate and  
434 ammonium in the background aerosols has been emphasized-observed during recent campaigns in the  
435 remote Mediterranean atmosphere (e.g. Mallet et al., 2019). To our knowledge, no data are available  
436 on both P and N concentrations in Mediterranean aerosols. The lowest concentrations of P relative to  
437 N in aerosol particles in the Mediterranean ~~have been~~ were observed during the cruise (value, Fu et  
438 al., in prep.). The TDP concentrations were consistent with the average value of 8.4  $\mu\text{g L}^{-1}$  measured  
439 in African dust rain samples collected in Spain over the 1996-2008 period (Izquierdo et al., 2012).  
440 Inorganic phosphorus predominated in the dust-rich rain, whereas organic P was dominant in the  
441 background rain as the contribution of DOP to the TDP was 60% and 44% in Rain ION and Rain  
442 FAST, respectively. The DOP/TDP ratio presents a very large range in Mediterranean rains, spanning  
443 from 6% in Spanish dusty rain samples (Izquierdo et al., 2012) to 75-92% in rains from Crete Islands  
444 (Violaki et al., 2018). A reason for this wide range could be that Mediterranean European aerosols, as  
445 opposed to Saharan dust particles, are dominated by organic phosphorus compounds associated with  
446 bacteria (Longo et al., 2014).

Commented [RS(-S37)]: Wet +dry?



447

448 **Figure 5: Comparison of dissolved (D) and total (T) TMs concentrations along with data from 14 former studies carried**  
449 **out in to previous studies in the eastern and western Mediterranean Sea.**

450 The dissolved and total TMs concentrations in the PEACETIME rains were lower than those reported  
451 in coastal areas (eastern Basin: Özsoy and Örnektekin, 2009; Al-Momani et al., 1998; Kanellopoulou  
452 et al, 2001 and western Basin: Guieu et al., 1997; Guerzoni et al., 1999b; Chester et al., 1997; Losno,  
453 1989; Frau et al., 1996) (Fig. 5), notably especially for the background Rain ION. This suggests the  
454 probable effect of both local anthropogenic influence at coastal sites due to higher aerosol  
455 concentrations in comparison to the remote Mediterranean (Fu et al., in prep.) and due to the reduction  
456 of anthropogenic emission for some elements since most of the referenced works on coastal rainwaters  
457 date from the late 1990s. This is particularly true for Cd and Pb and Cd whose emissions have strongly  
458 decreased over the last decades, notably due to removal of lead in gasoline and reduction of coal  
459 combustion (Pacyna et al., 2007). This has resulted in a clear decrease in the particulate concentrations  
460 of these metals in the Mediterranean atmosphere (Migon et al., 2008), consistent with the fact that  
461 concentrations in the PEACETIME rains are one to two orders of magnitude lower than reported in

**Commented [RS(-538)]:** Are you comparing like with like here? You state that concentrations likely decrease offshore and, although emissions of TMs may have decreased, if the literature data is from coastal sites you don't have direct evidence for this decline over the open ocean. However, you could infer it from reductions in leaded fuel and coal combustion. Is the decreasing atmospheric input evident in the full depth water column samples? Perhaps this is what the Fu et al data shows but the reader can't check this as the reference is 'in prep'. Later you mention the Dulac thesis as evidence. This paragraph needs rewriting and making more concise in order to strengthen your final, important statement. As it stands, this section is too speculative.



462 the literature. For these metals, the discrepancy is also observed between the concentrations in our  
463 open-sea rain samples and the concentrations (state which elements) measured in three rains collected  
464 at sea in April 1981 (Dulac, 1986), confirming that the large decrease of concentrations could be  
465 related with-to the decrease of-in anthropogenic emissions. Thus, our results show the former  
466 literature data from before [year] cannot-should not be used as a current reference about-for coastal  
467 rain composition due to recent environmental mitigation on-of metals-TM emissions.

#### 468 4.1.2. Enrichment factors

469 Enrichment Factors (EF) and solubility values of TMs and P observed during the two rain events were  
470 very contrasted (Fig. 6). In Rain ION, almost all elements were significantly enriched relative to the  
471 earth upper continental crust (EF >10, and up to  $\sim 10^3$  for Cd and Zn), whereas in Rain FAST, only Zn  
472 (73), Cd (48) and Mo (15) were slightly-enriched. Only Ti, Fe, and Mn did not present a significant  
473 enrichment (EF < 10) in Rain ION, in agreement with previous studies in the Mediterranean  
474 environment showing that these metals are mainly associated with mineral dust in -atmospheric  
475 deposition (e.g., Guieu et al., 2010; Desboeufs et al., 2018). For both rains rain samples, the EF of  
476 Zn was on average five times higher than the EF found in the rains previously studied in rain samples  
477 from coastal sites (?) in the Mediterranean region (Özsoy and Örnektekin, 2009; Al-Momani et al.,  
478 1998; Losno, 1989). However, extremely high enrichments of Zn in rainwater have also been reported  
479 from island sites in the Mediterranean Sea, for example, by Frau et al. (1996) reported with a  
480 geometric mean EFs of about  $\sim 6500$  in both crust-rich and crust-poor rains from two sites in southern  
481 Sardinia, and Fu et al. (2017) also reported EF higher than  $> 1000$  for Zn in atmospheric bulk  
482 deposition in Lampedusa Island. The Zn EF at station ION is the same order of magnitude as at these  
483 island sites which suggests - something about the anthro background signal being high in the open  
484 Med.

485 The anthropogenic origin of particulate TMs and P concentrations in seawater have been reported  
486 by several studies on atmospheric deposition in the western Mediterranean (e.g., Guieu et al., 2010;  
487 Sandroni and Migon, 2002; Desboeufs et al., 2018). For example, Desboeufs et al. (2018) showed that  
488 there is a large contribution of anthropogenic combustion sources to the -P, Cr, V and Zn background  
489 deposition fluxes. Aerosol composition monitoring over the Mediterranean coastal area showed the  
490 role of land-based sources and ship traffic sources on TMs contents (Bove et al., 2016; Becagli et al.,  
491 2017). However, all these sampling sites were located in coastal areas, where it was difficult to  
492 discriminate the potential local influences. Here, even if the on-board atmospheric gas and particle  
493 measurements did not show a specific anthropogenic influence during the period of Rain ION, the  
494 particles scavenged by this rain presented a clear suggest an anthropogenic signature for all TMs

**Commented [RS(-S39):** Your rain was open ocean not coastal so doesn't really show that historical coastal TM concentrations are higher. The comparison is with the thesis. You could say that coastal values are not representative of open ocean values generally

**Commented [RS(-S40):** This section jumps around a bit, Rain ION then Rain FAST, the Rain ION again, then both, etc. It would be easier to read if one station was discussed and the other one contrasted to it

**Commented [RS(-S41):** Change to dust-rich and dust-poor

**Commented [RS(-S42):** Do you mean atmos bulk wet depo here? If so, for clarity best to just say rain. If bulk dry you need to state that too

**Commented [RS(-S43):** What do you mean here? To resolve the contribution of various local industries and shipping or local inputs from long range transport



495 except Ti, Fe and Mn. However for Fe and Mn, ~~an~~ the influence of non-crustal sources in Rain ION  
496 is visible through a clear increase in the EF values compared to FAST (Fig. 6). This means that even  
497 over remote the Med Sea, the chemical composition of background aerosol particles is likely  
498 continuously impacted by anthropogenic sources.

**Commented [RS(-S44)]:** These two sentences disagree with each other. Need to be reworded.

499 Moreover, the EF values of TMs for Rain FAST were significantly lower than for Rain ION (Fig. 6)  
500 but similar to Saharan rains (Guerzoni et al., 1999b; Özsoy and Örnektekin, 2009). The comparison  
501 between dust-rich and background rains generally reveals a net difference of concentrations (at least  
502 higher by a factor 3 in dust-rich), notably for Al, Fe, Mn and Cr (Guerzoni et al., 1999b; Özsoy and  
503 Örnektekin, 2009). Such contrast was indeed observed for Al, Fe and Mn in the PEACETIME rains  
504 (Fig. 5), but also for Cu and Pb. The combination of higher concentrations and EF values <10 found  
505 in Rain FAST confirm that the dust contribution was important on deposition fluxes of many TMs.

**Commented [RS(-S45)]:** How does this study compare to the factor of three increase in concs between background and dust influenced rains – use your values – and state how this would impact EFs – more Al drives down EFs, Al predominantly from dust, etc.

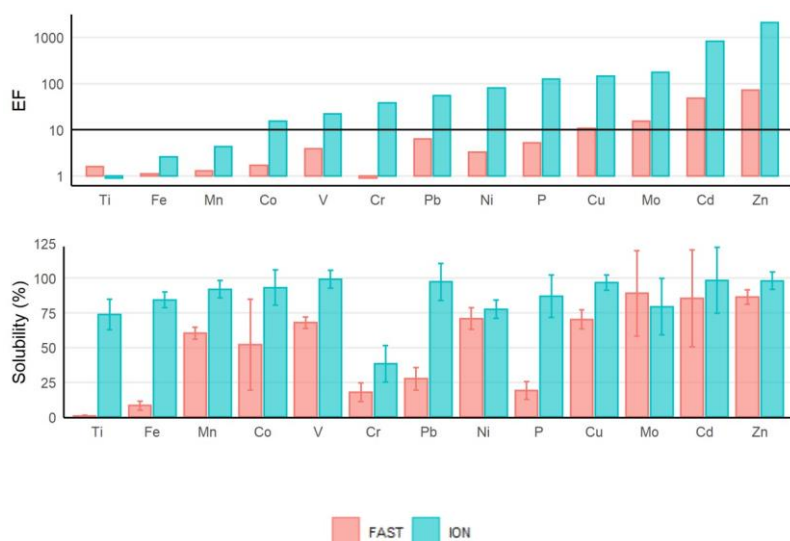
#### 506 4.1.3. Solubility

**Commented [RS(-S46)]:** Vague, just say that concs were higher and EFs suggest the reason for this was the impact of the dust plume. The EFs don't really tell us this. This section needs tightening up.

507 The solubility values were also larger higher in Rain ION than in the dusty Rain FAST, except for Mo  
508 for which the difference between both rain samples was not significant (Fig. 6). For Rain ION, TMs  
509 and P presented solubility higher than 78%, except for Cr (38%). In Rain FAST, solubility values  
510 <10% were observed for Al and Fe, more than 10 times lower than in Rain ION. For the other TMs,  
511 the highest difference in solubility was observed for Pb whose solubility decreased from 97% in Rain  
512 ION to 27% in Rain FAST. In a review on TMs solubility in Mediterranean rainwaters collected in  
513 coastal areas, Desboeufs (2021) emphasize the large range of solubility for all the TMs: Fe (0.8–41%),  
514 Cr (6–80%), Pb (5–90%), Ni (22–93%), Mn (16–95%), Cu (22–96%), Zn (14–99%), V (35–99%) and  
515 Cd (72–99%). The solubility ranges found in this study were generally consistent with those reviewed  
516 by Desboeufs (2021). In particular, the Mn solubility values in FAST (60%) and ION (92%) rains are  
517 close to those reported by Dulac (1986) from a dust-rich (57%) and an anthropogenic (83%) rain  
518 collected at sea in the Ligurian Sea and west of Sardinia in April 1981, respectively. Only Fe solubility  
519 (84%) found in Rain ION was higher than the average values previously reported. In the Rain FAST,  
520 Fe solubility was 8%, this is 10 times lower than the average Fe solubility in 10 dust-rich rains  
521 collected on the southeastern coast of Sardinia by Guerzoni et al. (1999b), but consistent with Saharan  
522 dust wet deposition collected in the Atlantic Ocean (Chance et al. 2015; Powell et al., 2015; Baker et  
523 al., 2017).

**Commented [RS(-S47)]:** Big target to hit!

**Commented [RS(-S48)]:** Can you suggest a reason for the difference?



524

525

526 **Figure 6: Enrichment Factors (EF, upper panel) and solubility (%), bottom panel) of phosphorus (P) and TMs ordered**  
 527 **by increasing EF in the two rainwater samples.**

528 Few studies have compared TMs solubility between dust-rich and background rains in the  
 529 Mediterranean. In Sardinia, Guerzoni et al. (1999b) observed an increase in solubility values from  
 530 dust-rich to background rains for Al, Cr, Fe and Pb (and hardly but only a slight increase for Cd), and  
 531 reported an inverse relationship between the particle concentration and solubility of Al, Fe, Pb and  
 532 Cd. Similarly, Theodosi et al. (2010) showed a decrease in TMs solubility with the increase in dust  
 533 load in rains collected on Crete Island. In those two studies, this-the magnitude of the decrease was  
 534 dependent-on-the-considered-metalspecific-to-the-TM, with Pb presenting the highest decrease in  
 535 solubility. The decrease in solubility from background to dust-rich rains was also-observed for P in  
 536 Spain (where?) by Izquierdo et al. (2012), with values of solubility decreasing from 25% to 7%, and  
 537 for Mn in offshore rains as mentioned above (Dulac, 1986).

538 /Metal partitioning in rainwater can be influenced by a number of parameters, such as pH, presence  
 539 of dissolved organic complexing ligands, in-cloud processinges, particle origin and load (Desboeufs  
 540 et al., 1999; Bonnet and Guieu, 2004; Paris and Desboeufs, 2013; Heimburger et al., 2013). However,  
 541 the particulate desert-mineral dust load, reflecting the dust vs-versus anthropogenic signature, is the  
 542 main control of TMs solubility in the Mediterranean rainwater (Özsoy and Ömektetin, 2009;

**Commented [RS(-S49):** Could you make the two panels the same size and the bars the same width?

**Commented [RS(-S50):** Could draw parallels with aero samples here, e.g. Jickells et al. (2016)

**Commented [RS(-S51):** Dust loading is only one proposed control and may not be a direct control – provide explanation e.g. perhaps the CaCO3 concentration is or the reduced impact of acidic gases, low RH, etc is – ref Baker et al., 2021



543 Theodosi et al., 2010). A much lower solubility of TMs in Rain FAST than in Rain ION (except for  
544 Mo) is consistent with the EFs in Rain FAST (Fig. 6), although no correlation between solubility and  
545 EF values could be observed. The case of Mo is unique, since its solubility was comparable in Rains  
546 ION and FAST despite a >20 times higher EF in Rain ION. As Mo solubility is seldom studied in the  
547 literature, we could not conclude on the reason for this particular outcome. It is interesting to note  
548 that despite the desert signature, the majority of metals have solubility greater than 50% in rain FAST.

#### 549 4.2. Atmospheric wet deposition as a source of TMs to the surface seawater

##### 550 4.2.1. Atmospheric fluxes

551 As mentioned before, the two collected rains were part of large rain systems, associated with patchy  
552 rainfalls that lasted several hours or days (section 3.1). This spatio-temporal variability led to  
553 heterogeneity in both rainwater concentrations and accumulated precipitation across the studied  
554 region. Such spatial variability has been observed by Chance et al. (2015) in the Atlantic Ocean.  
555 Moreover, even weak lateral advection can transfer surface water impacted by intense precipitation in  
556 the vicinity of the vessel. On this basis, the spatial extrapolation of wet deposition fluxes seems subject  
557 to a large uncertainty when the rain samples are not collected across the rain area (Chance et al.,  
558 2015). To best counteract this effect, spatial variability was taken into account to quantify the total  
559 precipitation i.e.  $3.5 \pm 1.2$  mm for rain ION and  $6.0 \pm 1.5$  mm for rain FAST (see 3.1) in order to  
560 quantify the wet deposition fluxes.

561 From the total (dissolved + particulate) Al concentration measured in the Rain FAST sample, we  
562 estimated the wet mineral dust deposition flux at  $65 \pm 18$  mg m<sup>-2</sup>, assuming 7.1% Al in dust (Guieu et  
563 al., 2002). The vertical distribution of dust particles (Fig. 2b) and the absence of high Al  
564 concentrations close to the sea surface (Fu et al., in prep.) indicate that dust dry deposition can be  
565 neglected. Based on the increase in total Al in the upper 20 m of the column water following the  
566 deposition events, Bressac et al. (2021) derived an average dust deposition flux of  $\sim 55$  mg m<sup>-2</sup> at  
567 FAST station which is comparable to our estimate. Although low compared to deposition fluxes  
568 reported in the western Mediterranean (Bergametti et al., 1989; Loÿe-Pilot and Martin, 1996; Temon  
569 et al., 2010), such our flux values estimates are among similar to the most intense weekly dust  
570 deposition fluxes recorded more recently in Corsica between 2011 and 2013 (range) and is  
571 equivalent to the mean weekly flux (value) observed in reported for Majorca Island during the same  
572 period (Vincent et al., 2016). The aerosol-columnar aerosol concentration during the dust event at the  
573 FAST station being was estimated to be between 0.18 and 0.24 g m<sup>-2</sup> (see Section 3.1.), the expected  
574 maximum values of atmospheric dust flux could be in this range. The comparison with the estimated

**Commented [RS(-S52)]:** Therefore, your data does not support this argument. Disagreement within statement. The EFs close to crustal TMs in RainFAST combined with the higher concentrations point to the role of mineral dust in reducing the fractional solubility of TMs in rainwater – or the presence of mineral dust overwhelms the background signal resulting in a net decrease in fractional solubility – although the net effect is the same, I favour the latter explanation

**Commented [RS(-S53)]:** Mo has a high conc in SW. If it has a predominantly marine source this could explain your uniform solubility. It would not explain your increase in EF necessarily but if there was an increase in seasalt aerosols it could do. You have the data to test this hypothesis

**Commented [RS(-S54)]:** Marine source? How reliable were the solubility data? Close to LoD and blanks?

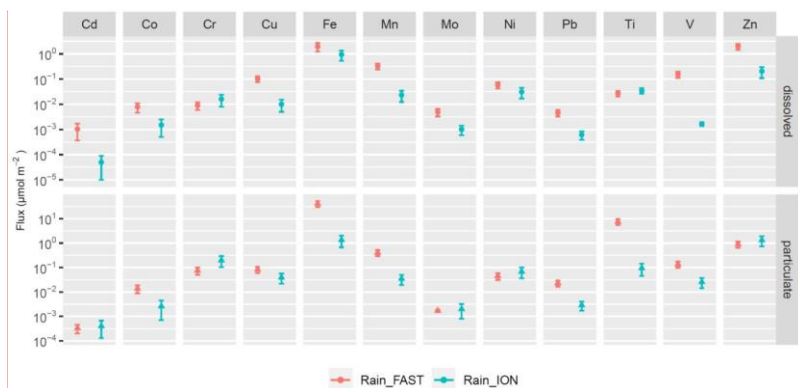
**Commented [RS(-S55)]:** How large?

**Commented [RS(-S56)]:** This is different than the Al proportion used in your EF calculations (Rudnick and Gao, 2003). Your EFs would be lower if you used concentrations based on 7.1% Al (Guieu et al., 2002) or your fluxes would be higher if you used the Rudnick and Gao (~ 8 %). It would be worth noting this variability. There is certainly an argument for using Saharan elemental ratios in your EF calcs (as discussed in Shelley et al. (2105)

**Commented [RS(-S57)]:** Fluxes aren't measured directly so reported, calculated or estimated are better words

**Commented [RS(-S58)]:** This is x3-4 higher than your flux estimates. A sentence to clarify why you support this view.

575 flux indicates that the atmospheric column was probably not totally washed-out by the short rain event.  
576 Indeed, Fig. 2b shows that a significant depolarization was observed immediately after the rain ended  
577 on the ship, before atmospheric advection could have brought dusty air possibly not affected by rain.  
578 Satellite products (Fig. S2) confirm that on 5 June, the dusty air mass was transported farther to the  
579 north-east from the station where it was replaced by clear air.



580  
581 **Figure 7: Dissolved (upper panels) and particulate (lower panels) wet deposition fluxes ( $\mu\text{mol m}^{-2}$ ) for**  
582 **the different TMs estimated from the two rains sampled on-board, considering the standard deviation**  
583 **on the TMs concentrations and the spatial variability of total precipitation over the area of sampling**  
584 **(Rain ION in blue and Rain FAST in red). Note different scales on the y axes.**

585 The atmospheric dissolved and particulate wet deposition fluxes of TMs, derived from the chemical  
586 composition of rain samples and total precipitation, are presented in Fig. 7. Co, Mo and Cd presented  
587 the lowest fluxes in the two rainfalls. Zn and Fe fluxes were on the same order of magnitude and were  
588 the highest dissolved fluxes compared to the other TMs in the two rains. The comparison showed that  
589 almost all the dissolved TMs fluxes were higher in the dusty rain, except Cr and Ti. For the particulate  
590 phase, the fluxes were mainly increased by the presence of mineral dust deposition for Co, Fe, Mn,  
591 Pb, Ti and V. Our results emphasized support previous studies that report that the presence of mineral  
592 dust deposition, even here in the case of a moderate deposition input flux reported here, enabled  
593 resulted in higher atmospheric inputs of TMs than from a low perturbed anthropogenic background  
594 rain. We found this to most notably be the case for dissolved Cd, Cu, Mn, V and Zn and for  
595 particulate Fe and Ti with more than one order of magnitude fluxes difference in input fluxes  
596 between the estimated from the two rain events. The orders of magnitude found in this study could  
597 be used as “typical a benchmark atmospheric fluxes” to estimate atmospheric inputs of TMs by a rain

**Commented [RS(-S59)]:** It would be useful to see the Al wet deposition flux as this is what you are using as the basis to estimate the bulk wet depo flux. It would also be nice to have a third panel showing the ratio or the Kd of dissolved to particulate TMs

**Commented [RS(-S60)]:** Explain how these two parameters differ. Are they not the same thing here?

**Commented [RS(-S61)]:** Explain why. They also have the greatest uncertainties – low concentrations and high blank contributions and >100% CRM recovery for Mo?

**Commented [RS(-S62)]:** Because these elements were primarily found in the particulate phase?

**Commented [RS(-S63)]:** Emphasised is stretching it for data from just two samples

**Commented [RS(-S64)]:** With the exception of Mn, these are predominantly considered pollution derived elements. It would be worth mentioning this.

**Commented [RS(-S65)]:** Poorly soluble, lithogenic elements. Al should also be reported here. I'm assuming it showed the same behaviour as Fe and Ti?

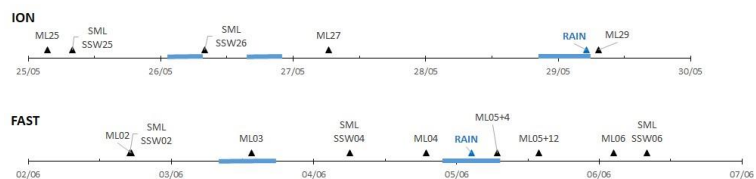
**Commented [RS(-S66)]:** Do you mean the range?



598 ~~event from wet deposition~~ to the western Med Sea. ~~However, w~~We must keep in mind, ~~however,~~ that  
599 annual and long-term deposition fluxes of ~~dust-related elements~~ (e.g. TERNON et al., 2010), but also  
600 nitrogen ~~species~~ (e.g., Richon et al., 2018b), ~~in the Med Sea,~~ are dominated by a few atypical, intense  
601 deposition events ~~in the Med Sea when they occurred, as is the case in many other oceanic regions~~  
602 ~~(Duce et al., 1991).~~

#### 603 4.2.2. Comparison between ~~TM<sub>s</sub>~~ wet deposition inputs and marine ~~stocks~~ at ION and FAST stations

604 ~~Our sampling strategy of Marine sampling sequences carried out collecting seawater~~ before and after  
605 ~~the rains were, to the best of~~ our knowledge, the first direct observations ~~intended~~ to trace the fate of  
606 atmospheric ~~metals-TMs~~ and nutrients in the water column after wet deposition ~~events~~. The time chart  
607 of the sampling of rain and column water (surface microlayer, subsurface seawater and mixed layer)  
608 is presented in Fig. 8. The impact of the two wet deposition ~~events~~ on nutrients ~~stocks~~ in the  
609 Mediterranean surface waters is discussed in ~~detail in~~ van Wanbeke et al. (2020) and Pulido-Villena  
610 et al. (2021). ~~To briefly summarise, b~~Both nitrate and DIP increased in the ML following the rains.  
611 Although the closure of the N and P budgets had to ~~necessarily~~ take into account post-deposition  
612 processes ~~such~~ as new nutrient transfer through the microbial food web (uptake, remineralisation, and  
613 adsorption/desorption processes on sinking particles), it was shown that wet deposition was a  
614 significant source of nutrients for ML during the cruise (~~roughly what %?~~). We focus here on the role  
615 of ~~TM<sub>s</sub>~~ wet deposition as a source of ~~metals-TMs~~ to the column water. To do so, we estimated the  
616 potential enrichment of ~~the SML~~ and ML from the rain by calculating the difference ( $\Delta$ ) in ~~TM<sub>s</sub>~~  
617 ~~stocks~~ before and after rains.



618  
619 **Figure 8: Sampling chronology during the ION and FAST stations for SML, SSW and ML. The blue**  
620 **periods correspond to rainfall in the station area (after ERA 5 reanalysis and radar imagery, see**  
621 **section 3.1). Samplings ~~were was~~ performed 4 days and 2 days before and 2 h after Rain ION, and at**  
622 **a higher frequency at the FAST station: 57, 37 and 7.5 hours before and 4.5, 12, 24 hours after Rain**  
623 **FAST. ~~SML and SSW samples could not be collected immediately before and after the rains because~~**  
624 **of bad weather conditions, and were collected 3 and 4 days before Rain ION, and 57 and 20 h before**  
625 **and 30 h after Rain FAST.**

**Commented [RS(-S67):** What does this mean? All elements discussed or only lithogenic elements?

**Commented [RS(-S68):** I'm wondering if concentrations or partitioning are a better choice of word than stocks (this applies throughout the paper)

**Commented [RS(-S69):** ... in an open ocean setting

**Commented [RS(-S70):** Move to Methods

**Commented [RS(-S71):** Move to methods

**Commented [RS(-S72):** Given how quickly the SML TM concentrations respond to atmospheric inputs and their relatively short residence times in the SML (hours – Ebling and Landing, 2015), how can you be sure that your SML sampling resolution was capturing the impact of the wet deposition events of the SML, especially given that wind speed (and sea state) is a critical factor in determining the integrity of the SML?



626 At ION, no SML sampling was done after rain, preventing the study of the rain effect. For the ML,  
627 the large variability in total and dissolved stocks between the two casts ML25 and ML27 before the  
628 rain makes the establishment of a background concentration levels before rain difficult. ML27 was  
629 used for the initial conditions since as it was the closest sampling from point to the post-rain  
630 measurements sample collection (ML29). As mentioned previously, dusty rain deposition over the  
631 FAST station area started on 3 June. Bressac et al. (2021) showed that the dust signature, traced by  
632 changes in Al and Fe stocks in the ML, was already visible from the ML03 sampling. We defined the  
633 enrichment of seawater layers as the difference between the maximum stocks after rain (from SML  
634 04 or 06 and ML05+4) and the initial seawater stocks (SML02 and ML02).

635 At ION, only particulate Cu (+27%) and Zn (+44%) stocks increased in the ML after the rain. Even if  
636 the dissolved forms of Cu and Zn predominated in the ML, this increase was accompanied by  
637 increasing Kd values, i.e. in the particulate/dissolved partitioning (0.07 vs 0.12 for Cu and 0.14 vs 0.2  
638 for Zn). This was also the case for Fe (Kd increased from 2.6 to 4.3), although no significant difference  
639 (<5%) was observed on the particulate Fe stock. The Kd values in the ION rain sample being higher  
640 than in the marine stock before the rain, that suggests the wet deposition at ION is mainly an additional  
641 source of particulate TMs.

642 At FAST, the ML stocks increased in the particulate phase for Fe (+61%), Mn (+15%) and Zn (+9%)  
643 and in the dissolved phase for Cu (+9%), Fe (+46%), Pb (+8%) and Zn (+15%) (Fig. 9). In addition  
644 to the marine inventories, the particulate TMs inputs by rain was also observed on Kd values and  
645 total X/Al in the ML. For example, Kd(Fe) increased from 0.14 to 0.17 in ML and its Kd was 0.25 in  
646 the rain. Even for Ni, for which no change in stock could be evidenced, Kd(Ni) decreased from 0.1 to  
647 0.07 and its Kd in the rain was 0.006. For Mn/Al, the Kd which fell from 0.27 before the rain to 0.008  
648 after the rain (ML05+4), in accordance with the rain ratio (0.004). In the SML, the dissolved and  
649 particulate stocks increased following rains for all TMs, from a factor 1.5 (Mo) to 10 (Fe) for the  
650 dissolved phase and from a factor 1.6 (Ni) to 67 (Fe) for the particulate phase (Fig. 9).

**Commented [RS(-S73)]:** As it reforms so quickly and rain disrupts it, how can you be sure that the SML sampled after the rain at FAST was in contact with the atmosphere and accumulating RW TMs?

**Commented [RS(-S74)]:** Suggesting that there was a surface advective current?

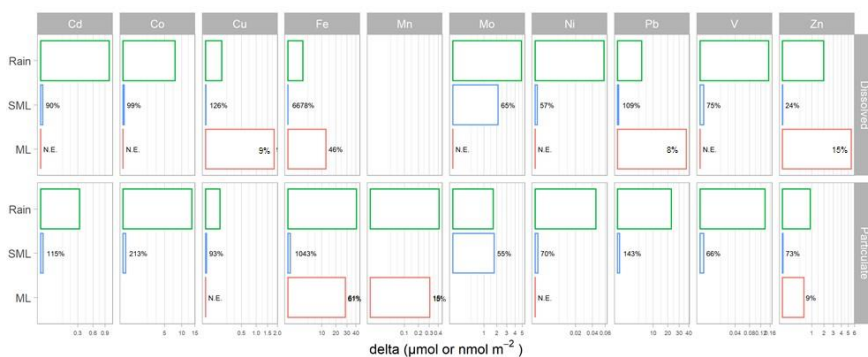
**Commented [RS(-S75)]:** Dissolved or particulate or both?

**Commented [RS(-S76)]:** I wonder if this is because of the mismatch between SML sampling and rosette casts.

**Commented [RS(-S77)]:** Additional to what?

**Commented [RS(-S78)]:** Particles scavenging dissolved TMs?

**Commented [RS(-S79)]:** Again, the SML samples may not have been representative of the wet depo inputs. In contrast, the ML likely was



652 **Figure 9: Comparison between TMs wet deposition fluxes (in green) and TMs marine stock deltas**  
 653 **(before and after the rain) in the SML (in blue) and in the ML (in red) at FAST. Dissolved = upper**  
 654 **panels and particulate = lower panels. Marine stocks increases are expressed in absolute values (Cd,**  
 655 **Co and Pb stocks in nmol m<sup>-2</sup>, and the other TMs in µmol m<sup>-2</sup>) and in relative values (%). N.E. = not**  
 656 **enhanced (increase <5%).**

657 The comparison between the observed enhancements in the SML stocks and the rain inputs at FAST  
 658 (Fig. 9) indicates that the atmospheric fluxes-inputs can explain support all observed deltas. Indeed,  
 659 the atmospheric particulate and dissolved fluxes of TMs were 2 to 4 orders of magnitude higher than  
 660 the mean stocks present in the SML, except Mo which was on the same order of magnitude. In the  
 661 ML, the magnitude of atmospheric particulate inputs was higher or similar to the particulate marine  
 662 delta of Fe, Mn and Zn. For Cu, Fe, Pb and Zn, the increase in dissolved stocks within the ML was 2  
 663 to 10 times higher than what be provided from the atmospheric inputs. As described in Guieu  
 664 et al. (2020), marine dynamic conditions at FAST were favourable to observe any change in the  
 665 water masses strictly attributed to external inputs coming from the atmosphere on a short time scale.  
 666 However, a cumulative effect of previous and surrounding wet deposition events could explain this  
 667 difference between atmospheric inputs from rain FAST and increase of marine dissolved stocks. We  
 668 cannot exclude the possibility of lateral transport of metals-TM from surrounding waters being  
 669 enriched by the rain events of 3 June 3 for example, as revealed by the increase in the 0-20 m Fe and  
 670 Al inventories (Bressac et al., 2021). Another hypothesis to explain that higher stock increases of  
 671 metals in the ML than the one derived from atmospheric deposition is related to post-deposition  
 672 processes. Indeed, once deposited, the atmospheric particulate fraction could still be partly solubilized  
 673 in seawater, as the solubilisation of TMs (e.g. Fe) could occur over several hours or days (Wagener et  
 674 al., 2008; Wuttig et al., 2013; Desboeufs et al., 2014). This could lead to an underestimate of the

**Commented [RS(-S80)]:** If we assume that the SML samples were representative of this layer before and after rain (and even if we don't), the similarity in Mo concentrations suggests to me that this element is not primarily delivered by atmospheric inputs

**Commented [RS(-S81)]:** From rain or total atmos depo?

**Commented [RS(-S82)]:** Days?

**Commented [RS(-S83)]:** Some ML residence time calculations could be of use here

**Commented [RS(-S84)]:** Many people have shown a delayed response of the dissolved pool to atmospheric inputs



675 dissolved TMs from atmospheric inputs. Moreover, the time lag between the rain and the first SML  
676 sampling (1 day) does not allow us to conclude on the role played by SML as a “trap” of the added  
677 dissolved metals by rain. However, results showed clearly the increase of dissolved TMs in the SML  
678 even 24 h after the rain (Fig. 9). Even if this increase could be due to dissolution processes (Tovar-  
679 Sanchez et al., 2020), we cannot exclude that the residence time of dissolved atmospheric TMs in the  
680 SML was sufficient to mask the atmospheric inputs in the ML05+4 sample. It is also known that  
681 dissolved concentrations in the ML are subject to various biological processes such as phytoplankton  
682 uptake (Morel et al., 2003). The comparison between ML05+4 and ML05+12 samples performed after  
683 the rain shows that the dissolved and particulate stocks decreased quickly for all the TMs (not shown),  
684 in agreement with the predominance of removal processes (sedimentation, biological transfer,  
685 adsorption) on these stocks. However, the rate of decrease depended on the TMs, showing that some  
686 removal processes predominate over others depending on the metal. For example, the dissolved metals  
687 TM decreases could correspond to scavenging onto particles, which is a common physico-chemical  
688 process occurring in the ocean for Fe (Wagener et al., 2010; Bressac and Guieu., 2013) or Co (Migon  
689 et al., 2020) and many other TMs.

690 /Finally, our results show that dusty wet deposition was a net source of all the studied trace metals  
691 for SML both in the dissolved and particulate fraction. For ML, atmospheric dust inputs were also a  
692 net source of particulate Fe, Mn, and Zn, and dissolved Cu, Fe, Pb and Zn. Due to various marine  
693 post-deposition processes, it was-is more complicated to observe the effect of wet deposition on  
694 dissolved stocks, explaining why the SML and ML particulate stocks were more impacted by rain  
695 than the dissolved stocks. On a timescale of hours, the Fe inventory was the most impacted by the  
696 dusty rain input, both in dissolved and particulate phases, confirming that the dust-rich rains are a net  
697 source of Fe to the surface Mediterranean Sea (Bonnet and Guieu, 2006, Bressac et al., 2021).

#### 698 4.2.3. Comparison between TMs wet atmospheric inputs and marine stocks at the scale in the Western 699 western and Central-central Mediterranean Sea

700 As observed from dissolved TMs stocks measured before and after the rains, a large part of the  
701 uncertainties in the data analysis results from various removal processes of TMs after wet deposition,  
702 which could have time resolution shorter than the sampling step. In order to limit the effect on-of these  
703 potential processes in-on data analysis, here we further study the role of wet deposition by comparing  
704 atmospheric dissolved fluxes to marine dissolved stocks by using TMs profiles in the ML at all 13  
705 marine stations, i.e. 22 ML samplings, throughout the whole cruise (Fig. 10). Indeed, considering that  
706 the collected rains were originating from large rain systems covering more than 50 000 km<sup>2</sup> around  
707 the sampling zone and were typical of Mediterranean wet deposition, we hypothesized that they could

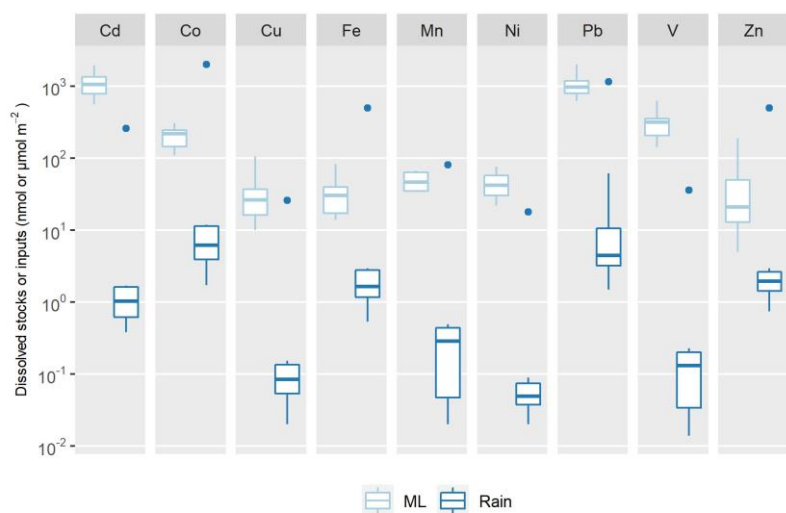
Commented [RS(-S85)]: It would be useful to see this – put in Supplementary Materials

Commented [RS(-S86)]: I'm not completely convinced it does because of the resolution problem. It certainly suggests it might given Tovar-Sanchez's findings of increases 24 h after rain but the signal is likely to be (significantly) diminished after this time.



708 have occurred in any of the explored areas during the cruise. Exceptional intense dust deposition  
709 events have been recorded in the Mediterranean, reaching  $20 \text{ g m}^{-2}$  (Bonnet et al., 2006). Sporadic and  
710 intense wet dust deposition higher than  $1 \text{ g m}^{-2}$  are regularly observed in the spring in the western  
711 Mediterranean basin (e.g., Vincent et al., 2016). At the beginning of the cruise, an intense wet dust  
712 deposition event (not collected) occurred over the South of Sardinia and over the Tyrrhenian Sea with  
713 fluxes reaching about  $9 \text{ g m}^{-2}$  (Bressac et al., 2021). In order to take into account the effect of such  
714 an event, we also estimated the atmospheric fluxes of dissolved ~~metals-TMs~~ based on a  $9 \text{ g m}^{-2}$  wet  
715 dust deposition event ~~considering-using~~ solubility values ~~found-in-the~~ estimated from rain-Rain FAST  
716 (Fig. 10). ~~The As [TM metal] solubility decreasing-decreases~~ with increasing dust load (Theodosi et al.,  
717 2010), this estimation constitutes probably a maximum value of the dissolved inputs of trace metals  
718 by such a dust deposition event. In addition to removal processes, the impact of rain inputs on TMs  
719 marine stocks is also controlled by MLD fluctuations ~~that-which~~ we ignored in ~~the-this~~ work ~~described~~  
720 ~~above~~ by using a fixed ML depth for the FAST and ION stations. ~~As However,~~ the variability of this  
721 MLD (7–21 m during the cruise, typical of Mediterranean thermal stratified period) could change the  
722 marine budgets by a factor of 3. ~~So we considered-used~~ the measured MLD (Van Wambeke et al.,  
723 2020) at each station for calculating the marine budgets of TM water budgets at each station.

**Commented [RS(-S87):** Which ones? Theodosi reports this for the TMs he studied but not your full suite. There are some that do, some that don't. See Jickells et al., 2016 and Baker et al., 2020. I appreciate these papers report data for the Atlantic rather than the Med but as they report data from Saharan and European air masses they are relevant.



724



725 **Figure 10: Comparison of marine stocks in the ML at all the stations occupied during the**  
726 **PEACETIME cruise with atmospheric inputs estimated (1) from ION and FAST rains (Boxesboxes)**  
727 **and (2) from an intense wet dust deposition event of  $9 \text{ g m}^{-2}$  (blue dots). Cd, Co and Pb stocks are in**  
728  **$\text{nmol m}^{-2}$ , and the other TMs in  $\mu\text{mol m}^{-2}$ . For Mn, marine stocks are derived from surface**  
729 **concentrations close to Corsica coasts (Wuttig et al., 2013: samples OUT at 0, 5 and 10 m) and in the**  
730 **Ionian Sea (Saager et al., 1993: Bannock basin at 0, 10, and 15 m), as no measurement is available**  
731 **from the PEACETIME cruise. Boxes and whiskers as in Fig. 4.**

732 Applying to the whole transect, the atmospheric inputs, obtained from our rain composition, were at  
733 least 100-fold smaller than the dissolved stocks in the mixed layer, except for Co, Fe and Zn. The  
734 atmospheric inputs represented more than 30% of the dissolved Zn stocks and 10 to 18% for Fe. This  
735 significant input of dissolved Fe is in agreement with our field observations in the ML. For  
736 Co, the maximum atmospheric fluxes estimated during the cruise represented  $>10\%$  of stocks. Here the  
737 comparison is based only on dissolved TMs in rain water, yet as discussed previously, the solubilisation  
738 post-deposition of atmospheric particles in the water column could further enrich the marine dissolved  
739 stocks. In the case of the intense dust deposition event, the dissolved inputs are of the same order of  
740 magnitude as marine stocks for Co, Fe, Mn, Pb and Zn. The enrichment in dissolved Fe and Mn was  
741 previously observed by Wuttig et al. (2013) after artificial dust seeding in large mesocosms (simulating  
742 a wet deposition event of  $10 \text{ g m}^{-2}$ ). The surface seawater could be significantly affected by the deposition  
743 of these dissolved elements in the case of wet dust deposition. ~~As (the marine TMs concentrations~~  
744 ~~measured during the cruise being were typical of Mediterranean surface seawater concentrations, we~~  
745 ~~conclude from these comparisons that wet deposition events, notably wet dust deposition events, prove~~  
746 ~~to beware~~ an external source of dissolved TMs for the Mediterranean Sea during the period of thermal  
747 stratification.

## 748 5. Conclusions

749 This study provides both the dynamical properties and chemical characterization of two ~~rainwaters~~  
750 ~~rain events collected~~ in the open Mediterranean Sea, concurrently with TM (list) ~~s~~ marine stocks in  
751 surface seawater. Our results are the only recent report of TM concentrations, EFs and fractional  
752 solubility values ~~for TMs~~ in rain samples collected in the remote Mediterranean Sea. By highlighting  
753 the discrepancy between TMs concentrations with ~~the previous offshore~~ and coastal rain studies, this  
754 work demonstrates the need to provide a new and recent database on ~~metal-TM~~ composition in  
755 Mediterranean rains in order to estimate the role of atmospheric TMs deposition. We ~~showed have~~  
756 ~~shown~~ the representativeness of ~~rain-Rain~~ FAST as typical of Saharan dust wet deposition ~~as well~~ in  
757 its chemical composition ~~as well~~ as in its magnitude and extent, whereas Rain ION is ~~a more~~-typical

Commented [RS(-S88)]: Only dissolved or dissolved and particulate?



758 ~~of an low-perturbed~~ anthropogenic background rain ~~of-for the~~ remote Mediterranean Sea. On this  
759 basis, we suggest ~~to use~~ using the chemical composition of PEACETIME rains as a new reference for  
760 ~~the~~ studies of TMs on wet deposition in ~~the~~ Mediterranean Sea.

761 Since atmospheric TMs have been identified as critical oligo-nutrients for ~~the~~ marine biosphere, ~~it is~~  
762 ~~important to study the response of the receiving waters to atmospheric inputs.~~ ~~our~~ This study is the  
763 first ~~to provide in situ~~ evidence that atmospheric wet deposition constitutes a significant external  
764 source for some of these elements to surface stratified Mediterranean seawater. ~~Our results show. We~~  
765 ~~recommend~~ that the original approach developed here ~~is very relevant in this purpose and could be~~  
766 used in other parts of the world where atmospheric ~~wet~~ deposition is ~~suspected-thought~~ to impact ~~the~~  
767 marine biosphere, ~~such as in~~ HNLC areas.

768

769 **Data availability.** Guieu et al., Biogeochemical dataset collected during the PEACETIME cruise.  
770 SEANOE. <https://doi.org/10.17882/75747> (2020). Atmospheric Data are accessible on  
771 <http://www.obsvlf.fr/proof/php/PEACETIME/peacetime.php>.  
772

773 **Author contributions.** KD and FF designed the study and wrote the manuscript; FF, ST, JFD, Ch.G made  
774 the on-board atmospheric measurements and sampling during the cruise; FF, ST and JD analysed the rain  
775 samples; MB, ATS, and ARR made the marine TMs sampling and analyses; PF was the reference scientist  
776 of PEGASUS, AF and FM managed all the technical preparation of atmospheric samplings, PC analysed  
777 the lidar data; KD, FD and Ce.G designed the cruise strategy; KD and Ce.G coordinated the PEACETIME  
778 project, FD coordinated the ChArMEx funding request, and near-real time and forecast survey of  
779 atmospheric conditions during the cruise; all the authors commented on the manuscript and contributed to  
780 its improvement.

781 **Competing interests.** The authors declare that they have no conflict of interest.

782 **Special issue statement.** This article is part of the special issue “Atmospheric deposition in the low-nutrient-  
783 low-chlorophyll (LNLC) ocean: effects on marine life today and in the future (ACP/BG inter- journal SI)”.  
784 It is not associated with a conference.

785 **Acknowledgements.** The authors wish to thank Thierry Alix the captain of the R/V *Pourquoi Pas ?* as well  
786 as the whole crew and technical staff for their involvement in the scientific operation. We gratefully thank  
787 Thibaut Wagener for his involvement in the trace-metals clean marine sampling and Mickaël Tharaud for  
788 the HR-ICP-MS analysis. We thank the Leosphere Technical support team and especially Alexandre  
789 Menard for their remote assistance with LIDAR repair under difficult off-shore conditions. H el ene Ferr e  
790 and the AERIS/SEDOO service are acknowledged for real-time collection during the cruise of maps from  
791 operational satellites and forecast models used in this study, with appreciated contributions of EUMETSAT

**Commented [RS(-S89)]:** How about an extra statement suggesting additional dry depo sampling to directly compare the inputs of wet and dry depo in future? Dry depo seems to have been overlooked in this study. What is thought to be the relative contribution of wet-dry dust depo events in the Med. Is wet depo thought to have a disproportionately large impact on TM seawater concs during stratification?



792 and AERIS/ICARE for MSG/SEVIRI products. EUMETNET is acknowledged for providing the  
793 panEuropean weather radar composite images through its OPERA programme. We acknowledge the US  
794 National Oceanic and Atmospheric Administration (NOAA) Air Resources Laboratory (ARL) for the  
795 provision of the HYSPLIT (HYbrid Single-Particle Lagrangian Integrated Trajectory) model via NOAA  
796 ARL READY website (<http://ready.arl.noaa.gov>) used in this publication. This study is a contribution to  
797 the PEACETIME project (<http://peacetime-project.org>; last accessed 05/04/2021), a joint initiative of the  
798 MERMEX and ChArMEX programmes supported by CNRS-INSU, IFREMER, CEA and Météo-France as  
799 part of the decadal meta-programme MISTRALS coordinated by CNRS-INSU. PEACETIME was endorsed  
800 as a process study by GEOTRACES and is also a contribution to IMBER and SOLAS international  
801 programs.

## 802 References

- 803 Achterberg, E. P., Braungardt, C. B., Sandford, R. C. and Worsfold, P. J.: UV digestion of seawater samples prior to the  
804 determination of copper using flow injection with chemiluminescence detection, *Anal. Chim. Acta*, 440, 27–36,  
805 [https://doi.org/10.1016/S0003-2670\(01\)00824-8](https://doi.org/10.1016/S0003-2670(01)00824-8), 2001.
- 806 Al-Momani, I. F., Aygun, S., and Tuncel, G.: Wet Deposition of Major Ions and TMs in the Eastern Mediterranean Basin, *J.*  
807 *Geophys. Res. (Atmos.)*, 103, 8287–8299, <https://doi.org/10.1029/97JD03130>, 1998.
- 808 Amato, F., Alastuey, A., Karanasiou, A., Lucarelli, F., Nava, S., Calzolari, G., Severi, M., Becagli, S., Gianelle, V. L.,  
809 Colombi, C., Alves, C., Custódio, D., Nunes, T., Cerqueira, M., Pio, C., Eleftheriadis, K., Diapouli, E., Reche, C.,  
810 Minguillón, M. C., Manousakas, M.-I., Maggos, T., Vratolis, S., Harrison, R. M., and Querol, X.: AIRUSE-LIFE+: a  
811 harmonized PM speciation and source apportionment in five southern European cities, *Atmos. Chem. Phys.*, 16, 3289–  
812 3309, <https://doi.org/10.5194/acp-16-3289-2016>, 2016.
- 813 Annett, A. L., Lapi, S., Ruth, T. J., and Maldonado, M. T.: The effects of Cu and Fe availability on the growth and Cu:C ratios  
814 of marine diatoms, *Limnol. Oceanogr.*, 53, 2451–2461, <https://doi.org/10.4319/lo.2008.53.6.2451>, 2008.
- 815 Avila, A., Queralt - Mitjans, I., and Alarcón, M.: Mineralogical composition of African dust delivered by red rains over  
816 northeastern Spain, *J. Geophys. Res. Atmos.*, 102, 21977–21996, <https://doi.org/10.1029/97JD00485>, 1997.
- 817 Bacconnais, I., Rouxel, O., Dulaquais, G., and Boye, M.: Determination of the copper isotope composition of seawater  
818 revisited: A case study from the Mediterranean Sea, *Chem. Geol.*, 511, 465–480,  
819 <https://doi.org/10.1016/j.chemgeo.2018.09.009>, 2019.
- 820 Baker, A. R., and Jickells, T. D.: Atmospheric deposition of soluble trace elements along the Atlantic Meridional Transect  
821 (AMT), *Prog. Oceanogr.*, 158, 41–51, <https://doi.org/10.1016/j.pocean.2016.10.002>, 2017.
- 822 Becagli, S., Anello, F., Bommarito, C., Cassola, F., Calzolari, G., Iorio, T. D., Sarra, A. D., Gómez-Amo, J. L., Lucarelli,  
823 F., Marconi, M., and Meloni, D.: Constraining the ship contribution to the aerosol of the central Mediterranean, *Atmosp.*  
824 *Chem. Phys.*, 17, 2067–2084, <https://doi.org/10.5194/acp-17-2067-2017>, 2017.
- 825 Bergametti, G., Gomes, L., Remoudaki, E., Desbois, M., Martin, D., and Buat-Ménard, P.: Present transport and  
826 deposition patterns of African dusts to the North-Western Mediterranean, in *Paleoclimatology and Paleometeorology:*  
827 *Modern and past patterns of global atmospheric transport*, Leinen, M., and Sarnthein, M., Eds., Springer, Dordrecht,  
828 NATO ASI Ser. C, 282, 227–252, [https://doi.org/10.1007/978-94-009-0995-3\\_9](https://doi.org/10.1007/978-94-009-0995-3_9), 1989.
- 829 Béthoux, J.P., Courau, P., Nicolas, E., and Ruiz-Pino, D.: Trace metal pollution in the Mediterranean Sea, *Oceanol. Acta* 13,  
830 481–488, <https://archimer.ifremer.fr/doc/00103/21418/> (last accessed 03 July 2021), 1990.
- 831 Bonnet, S. and Guieu, C.: Dissolution of atmospheric iron in seawater, *Geophys. Res. Lett.*, 31, L03303,  
832 <https://doi.org/10.1029/2003GL018423>, 2004.
- 833 Bonnet, S., and Guieu, C.: Atmospheric forcing on the annual iron cycle in the western Mediterranean Sea: A 1-year survey,  
834 *J. Geophys. Res.*, 111, C09010, <https://doi.org/10.1029/2005JC003213>, 2006.

<https://doi.org/10.5194/acp-2021-624>

Preprint. Discussion started: 25 August 2021

© Author(s) 2021. CC BY 4.0 License.



- 835 Bove, M. C., Brotto, P., Calzolari, G., Cassola, F., Cavalli, F., Fermo, P., Hjorth, J., Massabò, D., Nava, S., Piazzalunga,  
836 A., and Schembari, C.: PM<sub>10</sub> source apportionment applying PMF and chemical tracer analysis to ship-borne  
837 measurements in the Western Mediterranean, *Atmos. Environ.*, 125, 140–151,  
838 <https://doi.org/10.1016/j.atmosenv.2015.11.009>, 2016.
- 839 Bressac, M., and Guieu, C.: Post-depositional processes: What really happens to new atmospheric iron in the ocean's surface?,  
840 *Global Biogeochem. Cycles*, 27, 859–870, doi:10.1002/gbc.20076, 2013
- 841 Bressac, M., Wagener, T., Leblond, N., Tovar-Sánchez, A., Ridame, C., Albani, S., Guasco, S., Dufour, A., Jacquet, S.,  
842 Dulac, F., Desboeufs, K., and Guieu, C.: Subsurface iron accumulation and rapid aluminium removal in the  
843 Mediterranean following African dust deposition, *Biogeosciences Discuss.*, <https://doi.org/10.5194/bg-2021-87>, in  
844 review, 2021.
- 845 Bruland, K. W., Franks, R. P., Knauer, G. A. and Martin, J. H.: Sampling and analytical methods for the determination  
846 of copper, cadmium, zinc, and nickel at the nanogram per liter level in sea water, *Anal. Chim. Acta*, 105, 233–245,  
847 [https://doi.org/10.1016/S0003-2670\(01\)83754-5](https://doi.org/10.1016/S0003-2670(01)83754-5), 1979.
- 848 Buat-Ménard, P., and Chesselet, R.: Variable influence of the atmospheric flux on the trace metal chemistry of oceanic  
849 suspended matter, *Earth Planet. Sci. Lett.*, 42, 399–411, [https://doi.org/10.1016/0012-821X\(79\)90049-9](https://doi.org/10.1016/0012-821X(79)90049-9), 1979.
- 850 Buat-Ménard, P.: Particle geochemistry in the atmosphere and oceans, In: *Air-Sea Exchange of Gases and Particles*, Liss  
851 P.S., Slinn W.G.N. Editors, NATO ASI Series C, 108, 455–532, Springer, Dordrecht, [https://doi.org/10.1007/97894-009-7169-1\\_8](https://doi.org/10.1007/97894-009-7169-1_8), 1983.
- 853 Chance, R., Jickells, T. D. and Baker, A.R.: Atmospheric Trace Metal Concentrations, Solubility and Deposition Fluxes  
854 in Remote Marine Air over the South-East Atlantic, *Mar. Chem.*, 177, 45–56,  
855 <https://doi.org/10.1016/j.marchem.2015.06.028>, 2015.
- 856 Chazette, P., Flamant, C., Totems, J., Gaetani, M., Smith, G., Baron, A., Landsheere, X., Desboeufs, K., Doussin, J.F.,  
857 and Formenti, P.: Evidence of the complexity of aerosol transport in the lower troposphere on the Namibian coast during  
858 AEROCLO-sA, *Atmos. Chem. Phys.*, 19, 14979–15005, <https://doi.org/10.5194/acp-19-14979-2019>, 2019.
- 859 Chazette, P., Totems, J., Ancellet, G., Pelon, J., and Sicard, M.: Temporal consistency of lidar observations during aerosol  
860 transport events in the framework of the ChArMEx/ADRIMED campaign at Minorca in June 2013, *Atmos. Chem. Phys.*,  
861 16, 2863–2875, <https://doi.org/10.5194/acp-16-2863-2016>, 2016.
- 862 Chester, R., Nimmo, M., Corcoran, P. A.: Rain water-aerosol trace metal relationships at Cap Ferrat: a coastal site in the  
863 Western Mediterranean, *Mar. Chem.*, 58, 293–312, [https://doi.org/10.1016/S0304-4203\(97\)00056-X](https://doi.org/10.1016/S0304-4203(97)00056-X), 1997.
- 864 Desboeufs, K., Losno, R., Vimeux, F., Cholbi, S.: the pH-dependent dissolution of wind transported Saharan dust. *J. Geophys.*  
865 *Res.*, 104, 21287–21299, <https://doi.org/10.1029/1999JD900236>, 1999.
- 866 Desboeufs, K., Leblond, N., Wagener, T., Bon Nguyen, E., Guieu, C.: Chemical fate and settling of mineral dust in  
867 surface seawater after atmospheric deposition observed from dust seeding experiments in large mesocosms,  
868 *Biogeosciences*, 11, 5581–5594, <https://doi.org/10.5194/bg-11-5581-2014>, 2014.
- 869 Desboeufs, K., Bon Nguyen, E., Chevaillier, S., Triquet, S., and Dulac, F.: Fluxes and sources of nutrient and trace metal  
870 atmospheric deposition in the northwestern Mediterranean, *Atmos. Chem. Phys.*, 18, 14477–14492,  
871 <https://doi.org/10.5194/acp-18-14477-2018>, 2018.
- 872 Desboeufs, K.: Trace metals and contaminants deposition, in *Atmospheric Chemistry in the Mediterranean – Vol. 2,*  
873 *From Pollutant Sources to Impacts*, edited by Dulac, F., Sauvage, S., and Hamonou, E., Springer, Cham, Switzerland, in  
874 press, 2021.
- 875 Dulac, F.: Dynamique du transport et des retombées d'aérosols métalliques en Méditerranée occidentale, PhD Dissertation,  
876 Univ. Paris 7, 241 pp., 1986.

<https://doi.org/10.5194/acp-2021-624>

Preprint. Discussion started: 25 August 2021

© Author(s) 2021. CC BY 4.0 License.



- 877 Formenti, P., D'Anna, B., Flamant, C., Mallet, M., Piketh, S. J., Schepanski, K., Waquet, F., Auriol, F., Brogniez, G.,  
878 Burnet, F., Chaboureaud, J., Chauvigné, A., Chazette, P., Denjean, C., Desboeufs, K., Doussin, J., Elguindi, N., Feuerstein,  
879 S., Gaetani, M., Giorio, C., Klopfer, D., Mallet, M. D., Nabat, P., Monod, A., Solmon, F., Namwoonde, A., Chikwililwa,  
880 C., Mushi, R., Welton, E. J., and Holben, B.: The Aerosols, Radiation and Clouds in southern Africa field campaign in  
881 Namibia: Overview, illustrative observations, and way forward, *Bull. Am.Meteorol. Soc.*, 100, 1277–1298,  
882 <https://doi.org/10.1175/BAMS-D-17-0278.1>, 2019.
- 883 Frau, F., Caboi, R., and Cristini, A.: The impact of Saharan dust on TMs solubility in rainwater in Sardinia, Italy, In:  
884 The Impact of Desert Dust Across the Mediterranean, S. Guerzoni, and R. Chester (Eds.), Springer, Dordrecht, Environ. Sci.  
885 Technol. Library, 11, 285–290, [https://doi.org/10.1007/978-94-017-3354-0\\_28](https://doi.org/10.1007/978-94-017-3354-0_28), 1996.
- 886 Fu, Y.F., Desboeufs, K., Vincent, J., Bon Nguyen, E., Laurent, B., Losno, R., and Dulac, F.: Estimating chemical  
887 composition of atmospheric deposition fluxes from mineral insoluble particles deposition collected in the western  
888 Mediterranean region, *Atmos. Meas. Tech.*, 10, 4389–4401, <https://doi.org/10.5194/amt-10-4389-2017>, 2017.
- 889 Fu, F., Desboeufs, K., Triquet, S., Doussin J.-F., Giorio C., Chevaillier S., Feron A., Formenti, F., Maisonneuve F.,  
890 Riffault, V.: Aerosol characterisation and quantification of trace element atmospheric dry deposition fluxes in remote  
891 Mediterranean Sea during PEACETIME cruise, *Atmos. Chem. Phys.*, in prep.
- 892 Gallisai, R., Peters, F., Volpe, G., Basart., and Baldasano J. M.: Saharan Dust deposition may affect phytoplankton  
893 growth in the Mediterranean S. Sea at ecological time scales, *PLoS One*, 9, e110762,  
894 <https://doi.org/10.1371/journal.pone.0110762>, 2014.
- 895 Guerzoni, S. E. Molinaroli, P. Rossini, G. Rampazzo, G. Quarantotto, S. Cristini.: Role of desert aerosol in metal fluxes in the  
896 Mediterranean area, *Chemosphere*, 39, 229–246, [https://doi.org/10.1016/S0045-6535\(99\)00105-8](https://doi.org/10.1016/S0045-6535(99)00105-8), 1999b.
- 897 Guieu, C., and Ridame, C., Impact of atmospheric deposition on marine chemistry and biogeochemistry, in: *Atmospheric  
898 Chemistry in the Mediterranean - Vol. 2. From Air Pollutant Sources to Impacts*, edited by Dulac, F., Sauvage, S., and  
899 Hamonou, E., Springer, Cham, Switzerland, in press, 2021.
- 900 Guieu, C., Chester, R., Nimmo, M., Martin, J. M., Guerzoni, S., Nicolas, E., Mateu, J., and Keyse, S.: Atmospheric input  
901 of dissolved and particulate metals to the North Western Mediterranean, *Deep Sea Res. II*, 44, 655–674,  
902 [https://doi.org/10.1016/S0967-0645\(97\)88508-6](https://doi.org/10.1016/S0967-0645(97)88508-6), 1997.
- 903 Guieu, C., Loye-Pilot, M. D., Ridame, C., and Thomas, C.: Chemical Characterization of the Saharan dust endmember:  
904 Some biogeochemical implications for the Western Mediterranean Sea, *J. Geophys. Res.*, 107, 4258,  
905 <https://doi.org/10.1029/2001JD000582>, 2002.
- 906 Guieu, C., Bonnet, S., Wagener, T., and Loye-Pilot, M.-D.: Biomass burning as a source of dissolved iron to the open ocean?,  
907 *Geophys. Res. Lett.*, 32, L19608, <https://doi.org/10.1029/2005GL022962>, 2005.
- 908 Guieu, C. M.-D. Loye-Pilot, L. Benyahya, A. Dufour.: Spatial variability of atmospheric fluxes of metals (Al, Fe, Cd,  
909 Zn and Pb) and phosphorus over the whole Mediterranean from a one-year monitoring experiment: Biogeochemical  
910 implications, *Mar. Chem.*, 120, 164–178, <https://doi.org/10.1016/j.marchem.2009.02.004>, 2010.
- 911 Guieu, C., D'Ortenzio, F., Dulac, F., Taillandier, V., Doglioli, A., Petrenko, A., Barrillon, S., Mallet, M., Nabat, P., and  
912 Desboeufs, K.: Introduction: Process studies at the air-sea interface after atmospheric deposition in the Mediterranean  
913 Sea – objectives and strategy of the PEACETIME oceanographic campaign (May–June 2017), *Biogeosciences*, 17, 5563–  
914 5585, <https://doi.org/10.5194/bg-17-5563-2020>, 2020.
- 915 Hardy, J. T.: The sea surface microlayer: biology, chemistry and anthropogenic enrichment, *Prog. Oceanogr.*, 11, 307–328,  
916 [https://doi.org/10.1016/0079-6611\(82\)90001-5](https://doi.org/10.1016/0079-6611(82)90001-5), 1982.
- 917 Heimbürger, L. E., Migon, C., Dufour, A., Chiffolleau, J. F., and Cossa, D.: Trace metal concentrations in the  
918 Northwestern Mediterranean atmospheric aerosol between 1986 and 2008: Seasonal patterns and decadal trends, *Sci.  
919 Total Environ.*, 408, 2629–2638, <https://doi.org/10.1016/j.scitotenv.2010.02.042>, 2010.

<https://doi.org/10.5194/acp-2021-624>

Preprint. Discussion started: 25 August 2021

© Author(s) 2021. CC BY 4.0 License.



- 920 Heimburger, A., Losno, R., Triquet, S., Dulac F., and Mahowald, N. M.: Direct measurements of atmospheric iron, cobalt  
921 and aluminium-derived dust deposition at Kerguelen Islands, *Global Biogeochem. Cycles*, 26, GB4016,  
922 <https://doi.org/10.1029/2012GB004301>, 2012.
- 923 Heimburger, A., Losno, R., and Triquet, S.: Solubility of iron and other trace elements in rainwater collected on the  
924 Kerguelen Islands (South Indian Ocean), *Biogeosciences*, 10, 6617–6628, <https://doi.org/10.5194/bg-10-6617-2013>,  
925 2013.
- 926 Hersbach, H., Bell, B., Berrisford, P., Biavati, G., Horányi, A., Muñoz Sabater, J., Nicolas, J., Peubey, C., Radu, R.,  
927 Rozum, I., Schepers, D., Simmons, A., Soci, C., Dee, D., Thépaut, J.-N.: ERA5 hourly data on single levels from 1979  
928 to present, Copernicus Climate Change Service (C3S) Climate Data Store (CDS),  
929 <https://doi.org/10.24381/cds.adbb2d47>, 2018.
- 930 Herut, B., Krom, M. D., Pan, G., and Mortimer, R.: Atmospheric input of nitrogen and phosphorus to the Southeast  
931 Mediterranean: Sources, fluxes, and possible impact, *Limnol. Oceanogr.*, 44, 1683–1692,  
932 <https://doi.org/10.4319/lo.1999.44.7.1683>, 1999.
- 933 Hydes, D.J., and Liss, P.S.: Fluorimetric method for the determination of low concentrations of dissolved aluminium in  
934 natural waters, *Analyst*, 101, 922–931, 1976.
- 935 Gonzalez, L., and Briottet, X.: North Africa and Saudi Arabia day/night sandstorm survey (NASCube). *Remote Sens.*, 9,  
936 896, <https://doi.org/10.3390/rs9090896>, 2017.
- 937 Izquierdo, R., Benítez-Nelson, C. R., Masqué, P., Castillo, S., Alastuey, A., Castillo, S., Alastuey, A., and Avila, A.:  
938 Atmospheric phosphorus deposition in a near-coastal rural site in the NE Iberian Peninsula and its role in marine  
939 productivity, *Atmos. Environ.*, 49, 361–370, <https://doi.org/10.1016/j.atmosenv.2011.11.007>, 2012.
- 940 Izquieta-Rojano, S., García-Gomez, H., Aguilauume, L., Santamaría, J. M., Tang, Y. S., Santamaría, C., Valiño, F.,  
941 Lasheras, E., Alonso, R., Ávila, A., Cape, J. N., and Elustondo, D.: Throughfall and bulk deposition of dissolved organic  
942 nitrogen to holm oak forests in the Iberian Peninsula: flux estimation and identification of potential sources, *Environ.*  
943 *Pollut.*, 210, 104–112, <https://doi.org/10.1016/j.envpol.2015.12.002>, 2016.
- 944 Jordi, A., Basterretxea, G., Tovar-Sánchez, A., Alastuey, A. and Querol, X.: Copper aerosols inhibit phytoplankton  
945 growth in the Mediterranean Sea, *Proc. Nat. Acad. Sci.*, 109, 21246–21249, <https://doi.org/10.1073/pnas.1207567110>,  
946 2012.
- 947 Kanakidou, M., Mihalopoulos, N., Kindap, T., Im, U., Vrekoussis, M., Gerasopoulos, E., Dermizaki, E., Unal, A.,  
948 Koçak, M., Markakis, K., Melas, D., Kouvarakis, G., Youssef, A. F., Richter, A., Hatzianastassiou, N., Hilboll, A.,  
949 Ebojje, F., Wittrock, F., von Savigny, C., Burrows, J. P., Ladstaetter-Weissenmayer, A., and Moubasher, H.: Megacities  
950 as hot spots of air pollution in the East Mediterranean, *Atmos. Environ.*, 45, 1223–1235,  
951 <https://doi.org/10.1016/j.atmosenv.2010.11.048>, 2011.
- 952 Kanellopoulou, E. A.: Determination of heavy metals in wet deposition of Athens, *Global NEST J.*, 3, 45–50,  
953 <https://doi.org/10.30955/gnj.000181>, 2001.
- 954 Longo, A. F., Ingall, E. D., Diaz, J. M., Oakes, M., King, L. E., Nenes, A., Mihalopoulos, N., Violaki, K., Avila, A.,  
955 Benitez-Nelson, C. R., Brandes, J., McNulty, I., and Vine, D. J.: P-NEXFS analysis of aerosol phosphorus delivered to  
956 the Mediterranean Sea, *Geophys. Res. Lett.*, 41, 4043–4049, <https://doi.org/10.1002/2014GL060555>, 2014.
- 957 Losno, R.: Chimie d'éléments minéraux en traces dans les pluies méditerranéennes, Ph.D. thesis, Univ. Paris-Diderot de  
958 Paris 7, <https://tel.archives-ouvertes.fr/tel-00814327/document> (last accessed 4 July 2021), 1989.
- 959 Loÿe-Pilot, M.-D., and Martin, J. M.: Saharan dust input to the western Mediterranean: an eleven years record in Corsica,  
960 , In: *The Impact of Desert Dust Across the Mediterranean*, Guerzoni, S., Chester, R. (Eds.), Springer, Dordrecht, *Environ.*  
961 *Sci. Technol. Library*, 11, 191–199, [https://doi.org/10.1007/978-94-017-3354-0\\_18](https://doi.org/10.1007/978-94-017-3354-0_18), 1996.

<https://doi.org/10.5194/acp-2021-624>

Preprint. Discussion started: 25 August 2021

© Author(s) 2021. CC BY 4.0 License.



- 962 Mackey, K. R. M., Buck, K. N., Casey, J. R., Cid, A., Lomas, M. W., Sohrin, Y., and Paytan, A.: Phytoplankton  
963 Responses to Atmospheric Metal Deposition in the Coastal and Open-Ocean Sargasso Sea, *Front. Microbiol.*, 3, 359,  
964 <https://doi.org/10.3389/fmicb.2012.00359>, 2012.
- 965 Mallet, M. D., D'Anna, B., Mème, A., Bove, M. C., Cassola, F., Pace, G., Desboeufs, K., Di Biagio, C., Doussin, J.-F.,  
966 Maille, M., Massabò, D., Sciare, J., Zapf, P., di Sarra, A. G., and Formenti, P.: Summertime surface PM<sub>1</sub> aerosol  
967 composition and size by source region at the Lampedusa island in the central Mediterranean Sea, *Atmos. Chem. Phys.*,  
968 19, 11123–11142, <https://doi.org/10.5194/acp-19-11123-2019>, 2019.
- 969 Markaki, Z., Loëe-Pilot, M. D., Violaki, K., Benyahya, L., and Mihalopoulos, N.: Variability of atmospheric deposition  
970 of dissolved nitrogen and phosphorus in the Mediterranean and possible link to the anomalous seawater N/P ratio, *Mar.*  
971 *Chem.*, 120, 187–194, <https://doi.org/10.1016/j.marchem.2008.10.005>, 2010.
- 972 Migon, C., Robin, T., Dufour, A., and Gentili, B.: Decrease of lead concentrations in the Western Mediterranean  
973 atmosphere during the last 20 years, *Atmos. Environ.*, 42, 815–821, <https://doi.org/10.1016/j.atmosenv.2007.10.078>,  
974 2008.

<https://doi.org/10.5194/acp-2021-624>

Preprint. Discussion started: 25 August 2021

© Author(s) 2021. CC BY 4.0 License.



- 961 Migon, C., Heimbürger-Boavida, L.-E., Dufour, A., Chiffolleau, J.-F., and Cossa, D.: Temporal variability of dissolved 962 trace metals at the DYFAMED time-series station, Northwestern Mediterranean, *Mar. Chem.*, 225, 103846, 963 <https://doi.org/10.1016/j.marchem.2020.103846>, 2020.
- 964 Milne, A., Landing, W., Bizimis, M., and Morton, P.: Determination of Mn, Fe, Co, Ni, Cu, Zn, Cd and Pb in seawater 965 using high resolution magnetic sector inductively coupled mass spectrometry (HR-ICP-MS), *Analytica Chimica Acta*, 966 665, 200–207, <https://doi.org/10.1016/j.aca.2010.03.027>, 2010.
- 967 Morel, F. M. M., Hudson, R. J. M., and Price, N. M: Limitation of productivity by trace metals in the sea, *Limnol.* 968 *Oceanogr.*, 36, 1742–1755, <https://doi.org/10.4319/lo.1991.36.8.1742>, 1991.
- 969 Morel, F. M., Milligan, A. J., & Saito, M. A. Marine bioinorganic chemistry: the role of trace metals in the oceanic 970 cycles of major nutrients. *Treatise on geochemistry*, 6, 625, <https://doi.org/10.1016/B0-08-043751-6/06108-9>, 2003.
- 971 Morin, E., Krajewski, W. F., Goorich, D. C., Gao, X., and Sorooshian, S.: Estimating rainfall intensities from weather 972 radar data: The scale-dependency problem, *J. Hydrometeorol.*, 4, 782–797, [https://doi.org/10.1175/1525-9737-541\(2003\)004<0782:ERIFWR>2.0.CO;2](https://doi.org/10.1175/1525-9737-541(2003)004<0782:ERIFWR>2.0.CO;2), 2003.
- 974 Morley, N. H., Burton, J. D., Tankere, S. P. C., and Martin, J.-M.: Distribution and behaviour of some dissolved trace 975 metals in the western Mediterranean Sea, *Deep Sea Res. II*, 44, 675–691, [https://doi.org/10.1016/S0967-976\(1996\)00098-7](https://doi.org/10.1016/S0967-976(1996)00098-7), 1997.
- 977 Nehir, M., and Koçak, M.: Atmospheric water-soluble organic nitrogen (WSON) in the eastern Mediterranean: origin 978 and ramifications regarding marine productivity, *Atmos. Chem. Phys.*, 18, 3603–3618, <https://doi.org/10.5194/acp-18-3603-2018>, 2018.
- 980 Ochoa-Hueso, R., Allen, E. B., Branquinho, C., Cruz, C., Dias, T., Fenn, M. E., Manrique, E., Perez-Corona, M. E., 981 Sheppard, L. J., and Stock, W. D.: Nitrogen deposition effects on Mediterranean-type ecosystems: an ecological 982 assessment, *Environ. Pollut.*, 159, 2265–2279, <https://doi.org/10.1016/j.envpol.2010.12.019>, 2011.
- 983 Özsoy, T., and Örnektekin, S.: TMs in Urban and Suburban Rainfall, Mersin, Northeastern Mediterranean, *Atmos. Res.*, 984 94, 203–219, <https://doi.org/10.1016/j.atmosres.2009.05.017>, 2009.
- 985 Pacyna, E. G., Pacyna, J. M., Fudala, J., Strzelecka-Jastrzab, E., Hlawiczka, S., Panasiuk, D., Nitter, S., Pregger, T., 986 Pfeiffer, H., and Friedrich, R.: Current and future emissions of selected heavy metals to the atmosphere from 987 anthropogenic sources in Europe, *Atmos. Environ.*, 41, 8557–8566, <https://doi.org/10.1016/j.atmosenv.2007.07.040>, 2007.
- 989 Paris, R., and Desboeufs, K. V.: Effect of atmospheric organic complexation on iron-bearing dust solubility, *Atmos.* 990 *Chem. Phys.*, 13, 4895–4905, <https://doi.org/10.5194/acp-13-4895-2013>, 2013.
- 991 Pinedo-González, P., Joshua West, A., Tovar-Sánchez, A., Duarte, C. M., Marañón, E., Cermeño, P., González, N., 992 Sobrino, C., Huete-Ortega, M., Fernández, A., López-Sandoval, D. C., Vidal, M., Blasco, D., Estrada, M., and Sañudo 993 Wilhelmy, S. A.: Surface distribution of dissolved trace metals in the oligotrophic ocean and their influence 994 on phytoplankton biomass and productivity, *Global. Biogeochem. Cycles*, 29, 1763–1781, 995 <https://doi.org/10.1002/2015GB005149>, 2015.
- 996 Powell, C. F., Baker, A. R., Jickells, T. D., Bange, H. W., Chance, R. J., and Yodanis, C.: Estimation of the atmospheric 997 flux of nutrients and trace metals to the eastern tropical North Atlantic Ocean, *J. Atmos. Sci.*, 72, 4029–4045, 998 <https://doi.org/10.1175/JAS-D-15-0011.1>, 2015.

<https://doi.org/10.5194/acp-2021-624>

Preprint. Discussion started: 25 August 2021

© Author(s) 2021. CC BY 4.0 License.



- 999 Pulido-Villena, E., Rérolle, V., and Guieu, C.: Transient fertilizing effect of dust in P-deficient LNLC surface ocean, 1000  
Geophys. Res. Lett., 37, L01603, <https://doi.org/10.1029/2009GL041415>, 2010.
- 1001 Pulido-Villena, E., Desboeufs, K., Djaoudi, K., Van Wambeke, F., Barrillon, S., Doglioli, A., Petrenko, A., Taillandier,  
1002 V., Fu, F., Gaillard, T., Guasco, S., Nunige, S., Triquet, S., and Guieu, C.: Phosphorus cycling in the upper waters of  
1003 the Mediterranean Sea (Peacetime cruise): relative contribution of external and internal sources, Biogeosciences  
1004 Discuss., <https://doi.org/10.5194/bg-2021-94>, in review, 2021.
- 1005 Rahn, K. A.: The Chemical Composition of the Atmospheric Aerosol, Tech. Rept., Graduate School of Oceanography, 1006  
Univ. Rhode Island, Kingston, RI, 265 pp., <https://books.google.fr/books?id=q-dOQAAMAAJ> (last accessed 04 July 1007  
2021), 1976.
- 1008 Raut, J.-C., and Chazette, P.: Assessment of vertically-resolved PM10 from mobile lidar observations, Atmos. Chem. 1009  
Phys., 9, 8617–8638, <https://doi.org/10.5194/acp-9-8617-2009>, 2009.
- 1010 Richon, C., Dutay, J.-C., Dulac, F., Wang, R., and Balkanski, Y.: Modeling the biogeochemical impact of atmospheric 1011  
phosphate deposition from desert dust and combustion sources to the Mediterranean Sea, Biogeosciences, 15, 2499– 1012 2524,  
<https://doi.org/10.5194/bg-15-2499-2018>, 2018a.
- 1013 Richon, C., Dutay, J.-C., Dulac, F., Wang, R., Balkanski, Y., Nabat, P., Aumont, O., Desboeufs, K., Laurent, B., Guieu,  
1014 C., and Raimbault, P.: Modeling the impacts of atmospheric deposition of nitrogen and desert dust-derived phosphorus  
1015 on nutrients and biological budgets of the Mediterranean Sea, Prog. Oceanogr., 163, 21–39, 1016  
<https://doi.org/10.1016/j.pocean.2017.04.009>, 2018b.
- 1017 Ridame, C., Le Moal, M., Guieu, C., TERNON, E., Biegala, I. C., L’Helguen, S., and Pujol-Pay, M.: Nutrient control of  
1018 N<sub>2</sub> fixation in the oligotrophic Mediterranean Sea and the impact of Saharan dust events, Biogeosciences, 8, 2773–  
1019 2783, <https://doi.org/10.5194/bg-8-2773-2011>, 2011.
- 1020 Royer, P., Chazette, P., Lardier, M., and Sauvage, L.: Aerosol content survey by mini N<sub>2</sub>-Raman lidar: Application to 1021  
local and long-range transport aerosols, Atmos. Environ., 45, 7487–7495,  
1022 <https://doi.org/10.1016/j.atmosenv.2010.11.001>, 2011.
- 1023 Rudnick, R. L., and Gao, S.: Composition of the Continental Crust. In: Treatise on Geochemistry, Holland, H. D., and  
1024 Turekian, K. K. (Editors), Elsevier, Amsterdam. 3, 1–64, 2003.
- 1025 Saager, P. M., Schijf, J., and de Baar, H. J. W.: Trace-metal distributions in seawater and anoxic brines in the eastern 1026  
Mediterranean Sea, Geochim. Cosmochim. Acta, 57, 1419–1432, [https://doi.org/10.1016/0016-7037\(93\)90003-F](https://doi.org/10.1016/0016-7037(93)90003-F), 1027 1993.
- 1028 Sandroni, V., and Migon, C.: Atmospheric deposition of metallic pollutants over the Ligurian Sea: labile and residual 1029  
inputs, Chemosphere, 47, 753–764, [https://doi.org/10.1016/S0045-6535\(01\)00337-X](https://doi.org/10.1016/S0045-6535(01)00337-X), 2002.
- 1030 Saltikoff, E., Haase, G., Delobbe, L., Gaussiat, N., Martet, M., Idziorek, D., Leijnse, H., Novák, P., Lukach, M., and 1031  
Stephan, K.: OPERA the Radar Project, Atmosphere, 10, 320, <https://doi.org/10.3390/atmos10060320>, 2019.
- 1032 Sciare, J., Bardouki, H., Moulin, C., and Mihalopoulos, N.: Aerosol sources and their contribution to the chemical 1033  
composition of aerosols in the Eastern Mediterranean Sea during summertime, Atmos. Chem. Phys., 3, 291–302, 1034  
<https://doi.org/10.5194/acp-3-291-2003>, 2003.
- 1035 Sherrell, R. M. and Boyle, E. A.: Zinc, chromium, vanadium and iron in the Mediterranean Sea, Deep Sea Res. A, 35,  
1036 1319–1334, [https://doi.org/10.1016/0198-0149\(88\)90085-4](https://doi.org/10.1016/0198-0149(88)90085-4), 1988.

<https://doi.org/10.5194/acp-2021-624>

Preprint. Discussion started: 25 August 2021

© Author(s) 2021. CC BY 4.0 License.



- 1037 Smedley, P. L., and Kinniburgh, D. G.: Molybdenum in natural waters: A review of occurrence, distributions and 1038 controls, *Appl. Geochem.* 84, 387–432, <http://dx.doi.org/10.1016/j.apgeochem.2017.05.008>, 2017.
- 1039 Stortini, A. M., Cincinelli, A., Degli Innocenti, N., Tovar-Sánchez, A. and Knulst, J.: 1.12 - Surface Microlayer, In: 1040 Comprehensive Sampling and Sample Preparation - Vol. 1: Sampling Theory and Methodology, Pawliszyn, J. (Ed.-in-1041 Chief), 223–246, Academic Press, Oxford, <https://doi.org/10.1016/B978-0-12-381373-2.00018-1>, 2012.
- 1042 Temon, E., Guieu, C., Loÿe-Pilot, M. D., Leblond, N., Bosc, E., Gasser, B., Miquel, J. C., Martin, J.: The impact of 1043 Saharan dust on the particulate export in the water column of the North Western Mediterranean Sea, *Biogeosciences*, 1044 7, 809–826, <https://doi.org/10.5194/bg-7-809-2010>, 2010.
- 1045 The Mermex Group, et al.: Marine ecosystems' responses to climatic and anthropogenic forcings in the Mediterranean, 1046 *Prog. Oceanogr.*, 91, 97–166, <https://doi.org/10.1016/j.pocean.2011.02.003>, 2011.
- 1047 Theodosi, C., Markaki, Z., Tselepidis, A., and Mihalopoulos, N.: The significance of atmospheric inputs of soluble and 1048 particulate major and TMs to the Eastern Mediterranean Sea, *Mar. Chem.* 120, 154–163, 1049 <https://doi.org/10.1016/J.MARCHEM.2010.02.003>, 2010.
- 1050 Thieuleux, F., Moulin, C., Bréon, F. M., Maignan, F., Poitou, J., and Tanré, D.: Remote sensing of aerosols over the 1051 oceans using MSG/SEVIRI imagery, *Ann. Geophys.*, 23, 3561–3568, <https://doi.org/10.5194/angeo-23-3561-2005>, 1052 2005.
- 1053 Tovar-Sánchez, A., Arrieta, J. M., Duarte, C. M., and Sañudo-Wilhelmy, S. A.: Spatial gradients in trace metal 1054 concentrations in the surface microlayer of the Mediterranean Sea, *Front. Mar. Sci.*, 1, 79, 1055 <https://doi.org/10.3389/fmars.2014.00079>, 2014.
- 1056 Tovar-Sánchez, A., González-Ortegón, E., and Duarte, C. M.: Trace metal partitioning in the top meter of the ocean, 1057 *Sci. Total Environ.*, 652, 907–914, <https://doi.org/10.1016/j.scitotenv.2018.10.315>, 2019.
- 1058 Tovar-Sánchez, A., Rodríguez-Romero, A., Engel, A., Zäncker, B., Fu, F., Marañón, E., Pérez-Lorenzo, M., Bressac, 1059 M., Wagener, T., Triquet, S., Siour, G., Desboeufs, K., and Guieu, C.: Characterizing the surface microlayer in the 1060 Mediterranean Sea: trace metal concentrations and microbial plankton abundance, *Biogeosciences*, 17, 2349–2364, 1061 <https://doi.org/10.5194/bg-17-2349-2020>, 2020.
- 1062 Van Wambeke, F., Taillandier, V., Deboeufs, K., Pulido-Villena, E., Dinasquet, J., Engel, A., Marañón, E., Ridame, 1063 C., and Guieu, C.: Influence of atmospheric deposition on biogeochemical cycles in an oligotrophic ocean system, 1064 *Biogeosciences Discuss.*, <https://doi.org/10.5194/bg-2020-411>, in review, 2020.
- 1065 Vincent, J., Laurent, B., Losno, R., Bon Nguyen, E., Roulet, P., Sauvage, S., Chevaillier, S., Coddeville, P., 1066 Ouboulmane, N., di Sarra, A. G., Tovar-Sánchez, A., Sferlazzo, D., Massanet, A., Triquet, S., Morales Baquero, R., 1067 Fornier, M., Coursier, C., Desboeufs, K., Dulac, F., and Bergametti, G.: Variability of mineral dust deposition in the 1068 western Mediterranean basin and south-east of France, *Atmos. Chem. Phys.*, 16, 8749–8766, 1069 <https://doi.org/10.5194/acp-16-8749-2016>, 2016.
- 1070 Violaki, K., Bourrin, F., Aubert, D., Kouvarakis, G., Delsaut, N., and Mihalopoulos, N.: Organic phosphorus in 1071 atmospheric deposition over the Mediterranean Sea: An important missing piece of the phosphorus cycle, *Prog. Oceanogr.*, 163, 50–58, <https://doi.org/10.1016/j.pocean.2017.07.009>, 2018.
- 1073 Wagener, T., Pulido-Villena, E., and Guieu, C.: Dust iron dis-solution in seawater: Results from a one-year time-series 1074 in the Mediterranean Sea, *Geophys. Res. Lett.*, 35, L16601, <https://doi.org/10.1029/2008GL034581>, 2008.

<https://doi.org/10.5194/acp-2021-624>

Preprint. Discussion started: 25 August 2021

© Author(s) 2021. CC BY 4.0 License.



1075 Wagener, T., Guieu, C., and Leblond, N.: Effects of dust deposition on iron cycle in the surface Mediterranean Sea: 1076  
results from a mesocosm seeding experiment, *Biogeosciences*, 7, 3769–3781, <https://doi.org/10.5194/bg-7-3769-2010>,  
1077 2010.

1078 Wurl, O.: *Practical Guidelines for the Analysis of Seawater*, 1st ed., CRC Press., 2009.

1079 Wuttig, K., Wagener, T., Bressac, M., Dammshäuser, A., Streu, P., Guieu, C., and Croot, P. L.: Impacts of dust 1080  
deposition on dissolved trace metal concentrations (Mn, Al and Fe) during a mesocosm experiment, *Biogeosciences*,  
1081 10, 2583–2600, <https://doi.org/10.5194/bg-10-2583-2013>, 2013.

1082 Yoon, Y. Y., Martin, J.-M., and Cotté, M. H.: Dissolved trace metals in the western Mediterranean Sea: total 1083  
concentration and fraction isolated by C18 Sep-Pak technique, *Mar.*  
1084 *Chem.*, 66, 129–148, 1084 [https://doi.org/10.1016/S0304-4203\(99\)00033-X](https://doi.org/10.1016/S0304-4203(99)00033-X), 1999.

1085

1086



1087 **Figure Captions:**

1088

1089 Figure 1: Total precipitation (mm) between May 28 at 20:00 UTC and 29 at 10:00 UTC from ERA5 ECMWF  
1090 reanalysis. The red circle indicates the R/V position.

1091 Figure 2: On-board lidar-derived a) Apparent backscatter coefficient (ABC), (b) Temporal evolution (in  
1092 Local Time) of the lidar-derived volume depolarization ratio (VDR) where the dust plume is highlighted for 1093  
1094 values higher than ~1.7 (yellow to red colors) and the rain by values higher than 3 (indicated by the arrow),  
1095 and c) vertical profiles of the aerosol extinction coefficient (AEC) in cloud free condition, integrated over 3

1096 square (rms) variability along the time of the measurement. The dust layer is highlighted on the profiles.  
1097 The

1098 mean aerosol optical thickness is given in the boxed legend with its temporal variability (1 sigma). The  
1099 location of the marine boundary layer (MBL) is also pointed.

1100 Figure 3: Rain rates (mm/h) during the night between the 4 and 5 June, when Rain Fast was collected on  
1101 board, issued from European rain radar composites (OPERA programme) of June 5 between 00:00 and 02:45

1102 UTC.

1103 Figure 4: Boxplots of dissolved (left panels) and particulate (right panels) marine concentrations (pM) for  
1104 the different TMs within the ML (upper panels) and the SML (lower panels) at ION and FAST  
1105 stations. In the box plots, the box indicates the interquartile range, i.e. the 25<sup>th</sup> and the 75<sup>th</sup> percentile,  
1106 and the line within the box marks the median. The whiskers indicate the quartiles  $\pm 1.5$  times the  
1107 interquartile range. Points above and below the whiskers indicate outliers outside the 10<sup>th</sup> and 90<sup>th</sup>  
1108 percentile.

1109 Figure 5: Comparison of dissolved (D) and total (T) TMs concentrations along with data from 14 former  
1110 studies carried out in the eastern and western Mediterranean Sea.

1111 Figure 6: Enrichment Factors (EF, upper panel) and solubility (% , bottom panel) of phosphorus (P) and TMs  
1112 ordered by increasing EF in the two rainwater samples.

1113 Figure 7: Dissolved (upper panels) and particulate (lower panels) wet deposition fluxes ( $\mu\text{mol m}^{-2}$ ) for the  
1114 different TMs estimated from the two rains sampled on-board, considering the standard deviation on the TMs  
1115 concentrations and the spatial variability of total precipitation over the area of sampling (Rain ION in blue  
1116 and Rain FAST in red).

1117 Figure 8: Sampling chronology during the ION and FAST stations for SML, SSW and ML. The blue periods  
1118 correspond to rainfall in the station area (after ERA 5 reanalysis and radar imagery, see section 3.1).  
1119 Samplings were performed 4 days and 2 days before and 2 h after Rain ION, and at a higher frequency at the

<https://doi.org/10.5194/acp-2021-624>

Preprint. Discussion started: 25 August 2021

© Author(s) 2021. CC BY 4.0 License.



FAST station: 57, 37 and 7.5 hours before and 4.5, 12, 24 hours after Rain FAST. SML and SSW samples 1119 could not be collected immediately before and after the rains because of bad weather conditions, and were 1120 collected 3 and 4 days before Rain ION, and 57 and 20 h before and 30 h after Rain FAST.

1121 Figure 9: Comparison between TMs wet deposition fluxes (in green) and TMs marine stock delta (before 1122 and after the rain) in the SML (in blue) and in the ML (in red) at FAST. Dissolved = upper panels and 1123 particulate = lower panels. Marine stocks increase are expressed in absolute values (Cd, Co and Pb stocks in 1124  $\text{nmol m}^{-2}$ , and the other TMs in  $\mu\text{mol m}^{-2}$ ) and in relative values (%). N.E.: not enhanced (increase  $<5\%$ ).

1125 Figure 10: Comparison of marine stocks in the ML at all the stations occupied during the PEACETIME 1126 cruise with atmospheric inputs estimated (1) from ION and FAST rains (Boxes) and (2) from an intense wet 1127 dust deposition event of  $9 \text{ g m}^{-2}$  (blue dots). Cd, Co and Pb stocks are in  $\text{nmol m}^{-2}$ , and the other TMs in 1128  $\mu\text{mol m}^{-2}$ . For Mn, marine stocks are derived from surface concentrations close to Corsica coasts (Wuttig et al., 2013: samples OUT at 0, 5 and 10 m) and in the Ionian Sea (Saager et al., 1993: Bannock basin at 0, 10, 1130 and 15 m), as no measurement is available from the PEACETIME cruise. Boxes and whiskers as in Fig. 4.

1131